

EFFECTS OF NATURAL ORGANIC MATTER ON CONTAMINANT REMOVAL
BY SUPERFINE POWDERED ACTIVATED CARBON COUPLED WITH
MICROFILTRATION MEMBRANES

A Thesis
Presented to
the Graduate School of
Clemson University

In Partial Fulfillment
of the Requirements for the Degree
Master of Science
Environmental Engineering and Earth Sciences

by
Mengfei Li
May 2014

Accepted by:
Dr. David Ladner, Committee Chair
Dr. Tanju Karanfil
Dr. Cindy Lee

ABSTRACT

Hybrid activated carbon/membrane systems are used in drinking water treatment for their significant capability of removing synthetic organic contaminants (SOCs) or taste-and-odor compounds along with particles. Preliminary data showed that decreasing the carbon particle size and creating superfine powdered activated carbon (S-PAC) removed phenanthrene and atrazine better than adsorbents with larger particle size in the presence of competitive adsorbents like natural organic matter (NOM). NOM is present in all natural water from degradation of terrestrial biomass which leaches from soil into a water source. Water treatment facilities target the removal of NOM because they are precursors to disinfection by-products formed as a result of chlorination. The thesis addresses the effects of NOM on contaminant removal through different treatment techniques. The effect of NOM in the coupled S-PAC/microfiltration membrane process was investigated further in the study. Atrazine and carbamazepine were applied in the experiments as the SOCs. Filtered Edisto River water (about 4 mg/L dissolved organic carbon (DOC)) was applied in bench-scale membrane tests. Results indicated that the S-PAC had a better removal efficiency of both atrazine and carbamazepine than powdered activated carbon (PAC). In the presence of NOM, the dominance of S-PAC removal efficiency was more apparent than in deionized water. Flux measurements in deionized water showed that S-PAC caused about 50 percent flux decline; however, when NOM was present the flux decreased much further. NOM proved to be the main culprit in membrane fouling, not S-PAC. Instead of increasing the pore blockage, S-PAC actually decreased the fouling compared to NOM alone. Thus, this evidence helped alleviate some initial worries about the small particles in S-PAC

being detrimental to membrane systems. The results indicated that S-PAC may be applied in full-scale membrane plants and will perform better than conventional PAC. NOM concentration was varied and pH value was adjusted. Since the adsorption of contaminant decrease more rapidly on PAC when NOM concentration increases, the external sites and conformation on S-PAC may be more favorable for the SOCs. At low pH, carboxyl groups of NOM will be protonated that results in larger complexes that are easy to on adsorbents and harder to block the membrane.

DEDICATION

I would like to dedicate my thesis to my family, who have always been supportive of my endeavors.

ACKNOWLEDGEMENTS

I would like to acknowledge my advisor, Dr. David Ladner, who was willing to meet with me on a weekly basis to discuss my results and future experiments. I would also like to acknowledge Dr. Tanju Karanfil and Dr. Cindy Lee for their willingness to be members of my committee. Also, Dr. Karanfil helped me with useful guidance and support, and supplied the carbon used in this project.

I would like to acknowledge Anne Cummings for her support and help with the technical problems with HPLC, LSC, and UV/Vis. I am also very thankful to the former student, Jaelyn Ellerie, who supported lots of useful experiment results in her thesis and paper. I would like to acknowledge Onur Apul, Mahmut Ersan, and Erin Partlan for their help with the experiments especially with carbon characterization and usage. Especially thanks for Erin Partlan who gave me a lot of constructive comments in this project. I also want to acknowledge Semra Bakkaloglu, Na Hao, Muriel Steele, and Chen Chen for being generous to spend time and share their lab skills with Amicon cell, HPLC, LSC, and TOC analyzer. Also, I am thankful to Rui Xiao for sharing his lab supplies with me. I would like to thank Ying Tu and Pauline Amaral for their help when I was doing the experiments in the lab.

Materials and supplies for this project were provided through a grant from the National Science Foundation, CBET 1236070.

TABLE OF CONTENTS

Chapter 1 INTRODUCTION.....	1
Chapter 2 BACKGROUND.....	3
2.1 Activated carbon	3
2.1.1 Origin and Production.....	3
2.1.2 Applications	3
2.1.3 Factors Influencing Adsorption	4
2.2 Superfine Powdered Activated Carbon.....	7
2.3 Natural Organic Matter	8
2.4 Adsorbent/Membrane Systems	11
Chapter 3 RESEARCH OBJECTIVES	17
Chapter 4 MATERIALS AND METHODS	19
4.1 Adsorbents	19
4.1.1 Properties of adsorbents	19
4.2 Adsorbates.....	20
4.2.1 Atrazine.....	21
4.2.2 Carbamazepine.....	22
4.3 PAC/MF Experiments.....	23
4.3.1 Flux Decline Experiment	24
4.3.2 NOM Experiments	25
4.3.3 Calculation of Carbon Usage Rate.....	26
4.3.4 Empty Bed Contact Time and Bed Volume	27
4.3.5 Membrane Resistance	27
Chapter 5 RESULTS AND DISCUSSION	28
5.1 Flux Decline Experiments.....	28
5.1.1 Comparing flux decline between PAC and S-PAC	28
5.1.2 The effect of bath sonication.....	30
5.1.3 Comparison of probe sonication and bath sonication	31
5.1.4 The effect of sonication time on flux decline	32
5.1.5 The effect of sonication power on the flux decline.....	32
5.1.6 Comparison of flux decline with different adsorbents.....	33
5.1.7 Comparison of the effect of carbon addition method	34
5.1.8 Comparison of the effect of carbon mass	37
5.2 Competitive Adsorption between SOCs and NOM	39

5.2.1 Comparison of the adsorption capacity between coating technique and stirred cell technique	39
5.2.2 Comparison of the adsorption with and without NOM	40
5.2.3 Comparison of adsorption with different carbon	42
5.2.4 Flux data with and without NOM	45
5.2.5 Flux data for different carbons.....	46
5.2.6 Carbamazepine data.....	48
5.2.7 Effects of NOM concentration.....	50
5.2.8 Effects of pH.....	54
5.2.9. Caveats concerning contact times.....	59
Chapter 6 CONCLUSIONS AND RECOMMENDATIONS.....	61
6.1 Conclusions.....	61
6.2 Future Work.....	64
6.2.1 The effects of ionic strength	64
6.2.2 Aggregation research	64
6.2.3 Further experiments of pH effects	65
6.2.4 Modeling research.....	65
APPENDICES	66
APPENDIX A: Preparation of Radiolabeled Atrazine Stock Solution	67
APPENDIX B: The MDL of Radiolabeled Atrazine with C ¹⁴	69
APPENDIX C: Standard Operating Procedure of Amicon Cell.....	70
APPENDIX D: Front Panel of LabView Software Interface	72
APPENDIX E: The Correlation between Suwannee River NOM Concentration and TOC.....	73
APPENDIX F: Preparation and Storage of Standard Solutions	75
REFERENCES	79

LIST OF TABLES

Table 2.1 Factors Influencing Adsorption on Activated Carbon (9)	4
Table 2.2 Physical and chemical characteristics of humic substances (28).....	11
Table 4.1 Properties of the activated carbon materials investigated.....	20
Table 4.2 Particle size of different carbon	20
Table 4.3 Adsorbate Properties.....	22
Table 5.1 Membrane resistance data with different carbon addition methods	37
Table 5.2 EBCT, BV, and CUR with Norit 20B and WC 800. The EBCT is calculated by 90% removal of SOCs.	45

LIST OF FIGURES

Figure 2.1 Examples of oxygen and nitrogen-containing functional groups on an activated carbon surface. Adapted from references (9) and (10).	5
Figure 2.2 Fraction of NOM in surface water based on DOC (26).	9
Figure 2.3 Schematic of humic acid model structure (25).	10
Figure 2.4 Schematic of fulvic acid model structure (25).	10
Figure 4.1 Molecular structures of atrazine (a) and carbamazepine (b).	22
Figure 4.2 The bench-scale microfiltration setup (67).	24
Figure 5.1 Flux data with WPH PAC and WPH S-PAC with the pressure of 10 psi. The membrane was coated with 3 mg carbon. The average DDI water flux in the WPH PAC experiment was 2212 lmh and that in the WPH S-PAC experiment was 2106 lmh.	29
Figure 5.2 Flux data with WPH PAC and WPH S-PAC with and without bath sonication at the pressure of 10 psi. The membrane was coated with 3 mg carbon. The average DDI water fluxes were 2206, 2112, 2331, and 2015 lmh, respectively, for the experiments in the legend, top to bottom.	30
Figure 5.3 Flux data with WPH PAC and WPH S-PAC with bath sonication and probe sonication, separately, at the pressure of 10 psi. The membrane was coated 3 mg carbon. The average DDI water fluxes were 1897, 1985, 1910, and 1981 lmh, respectively.	31
Figure 5.4 Flux data with WPH S-PAC with different time periods of probe sonication at the pressure of 10 psi. The membrane was coated with 3 mg carbon. The average DDI water fluxes were 1970, 2081, 1908, 2050, and 1970, respectively.	32
Figure 5.5 Flux data with WPH S-PAC with probe sonication at different power levels. Pressure was 10 psi. The membrane was coated with 3 mg carbon. The average DDI water fluxes were 2129, 2175, and 1908, lmh, respectively.	33
Figure 5.6 Flux data with various S-PAC type at the pressure of 10 psi. The membrane was coated 3mg carbon. Probe sonication at 50% power and 5 minutes was performed before using. The average DDI water flux is 2283 lmh at experiment with WC 800, 2257 lmh at experiment with Norit 20B, 1987 lmh at experiment with WPH.	34
Figure 5.7 Flux data with WC 800 PAC and S-PAC added in Amicon cell and pressure vessel, separately, at the pressure of 10 psi. The carbon mass coated on the membrane was 3 mg. Probe sonication at 50% power and 5 minutes was performed	

before using. The feed solution contained methylene blue at 0.9 mg/L. The average DDI water flux was 1407 lmh for experiment with PAC in Amicon cell, 1952 lmh for experiment with PAC in pressure vessel, 2016 lmh for experiment with S-PAC in Amicon, and 1715 lmh for experiment with S-PAC in pressure vessel. 35

Figure 5.8 Flux data with WC 800 S-PAC added into Amicon cell and pressure vessel. The average DDI water flux was 2099 lmh at 1.5 mg steady addition, 2055 lmh at 3 mg steady addition, 2082 lmh at 6 mg steady addition, 2134 lmh at step addition with 1 mg coating, 2278 lmh at step addition with 3 mg coating. 37

Figure 5.9 Flux data with various S-PAC mass at the pressure of 10 psi. The carbon stock was probe sonicated at 50% power and 5minutes before using, and added into pressure vessel. The average DDI water flux was 2099 lmh for experiment with 3mg WC 800, 2055 lmh for experiment with 6mg WC 800, 2082 lmh for experiment with 12mg WC 800. 38

Figure 5.11 Comparison of atrazine removal using the membrane coating technique and the stirred cell technique for 1 mg of WC 800 in both PAC and S-PAC forms. The feed solution was radiolabeled atrazine at 15 ppb in Edisto River water with 4 ppm DOC. 40

Figure 5.12 Comparison of 1 mg of WC 800 in both PAC and S-PAC forms using the membrane coating technique. The feed solution was radiolabeled atrazine at 15 ppb in both Edisto water with 4 ppm DOC and DDI water. Duplicate results of the Edisto experiment are shown by the error bars (actual values for each replicate lie at the end of the error bars). 41

Figure 5.13 Comparison of the adsorption between WC 800 PAC and S-PAC forms using the membrane coating technique. The feed solution was radiolabeled atrazine at 150 ppb in Edisto water with 4 ppm DOC. 41

Figure 5.14 Comparison of WC 800 and Norit 20B in both PAC and S-PAC forms at 1 mg in the membrane coating technique. The feed solution was radiolabeled atrazine at 15 ppb in DDI water. 43

Figure 5.15 Comparison of WC 800 and Norit 20B in both PAC and S-PAC forms at 1 mg in the membrane coating technique. The feed solution was radiolabeled atrazine at 15 ppb in Edisto water with 4 ppm DOC. 44

Figure 5.16 Comparison of the normalized flux values for 1 mg of WC 800 in both PAC and S-PAC forms in the membrane coating technique. The feed solution was radiolabeled atrazine at 15 ppb in both Edisto water with 4 ppm DOC and in DDI water. 46

Figure 5.17 Comparison of normalized flux for 1 mg of WC 800 and Norit 20B in both PAC and S-PAC forms in the membrane coating technique. The feed solution was radiolabeled atrazine at 15 ppb in Edisto water with 4 ppm DOC. 47

Figure 5.18 Comparison of the WC 800 in both PAC and S-PAC forms with 1 mg in the membrane coating technique. The feed solution was carbamazepine at 1000 ppb in Edisto water with 4 ppm DOC..... 48

Figure 5.19 Comparison of WC 800 PAC and S-PAC (1 mg coating) for adsorbtion of atrazine and carbamazepine. The feed solution was atrazine at 15 ppb or carbamazepine at 1000 ppb in Edisto water with 4 ppm DOC..... 49

Figure 5.20 Comparison of WC 800 PAC and S-PAC (1 mg) with the membrane coating technique. The feed solution was carbamazepine at 1000 ppb in Edisto water with 4 ppm DOC and DDI water. 50

Figure 5.21 Comparison of atrazine removal by a 1 mg coating of WC 800 in both PAC and S-PAC forms with different SRNOM concentrations. The atrazine concentration was 15 ppb. 51

Figure 5.22 Comparison of NOM removal by 1 mg coatings of WC 800 PAC and S-PAC. The experiment was repeated for different SRNOM concentrations. The feed atrazine concentration was 15 ppb. These are the NOM data from the same experiments for which atrazine data were plotted in Figure 5.21. 52

Figure 5.23 Flux comparison for 1 mg coatings of WC 800 S-PAC with different SRNOM concentrations. The atrazine concentration was 15 ppb. 53

Figure 5.24 Comparison of flux decline for 1 mg of WC 800 PAC with different SRNOM concentrations using the membrane coating technique. The atrazine concentration was 15 ppb. 54

Figure 5.25 Atrazine removal comparison at different pH values for 1 mg of WC 800 S-PAC coatings in the presence of NOM. The atrazine and SRNOM concentrations were 15 ppb and 4 ppm DOC, respectively. 55

Figure 5.26 Atrazine removal for 1 mg coatings of WC 800 PAC with different pH in the presence of NOM. The feed atrazine concentration was 15 ppb in SRNOM with 4 ppm DOC. 56

Figure 5.27 NOM removal for a 1 mg coating of WC 800 S-PAC at varying pH. The atrazine concentration was 15 ppb in SRNOM with 4 ppm DOC. 57

Figure 5.28 NOM removal for 1 mg coatings of WC 800 PAC at varying pH. The atrazine concentration was 15 ppb in SRNOM with 4 ppm DOC. 57

Figure 5.29 Flux comparison for 1 mg coatings of WC 800 S-PAC at varying pH. The atrazine concentration was 15 ppb in SRNOM with 4 ppm DOC. 58

Figure 5.30 Flux comparison for 1 mg coatings of WC 800 PAC with varying pH. The atrazine concentration was 15 ppb in SRNOM with 4 ppm DOC. 59

LIST OF SYMBOLS AND ABBREVIATIONS

Abbreviations

BV	Bed Volume
CUR	Carbon Usage Rate
DBP	Disinfection by-product
DOC	Dissolved Organic Carbon
DOM	Dissolved Organic Matter
EBCT	Empty Bed Contact Time
FA	Fulvic Acid
FTIR	Fourier Transform Infrared Spectroscopy
GAC	Granular Activated Carbon
HA	Humic Acid
HPLC	High Performance Liquid Chromatography
HSDM	Homogeneous Surface Diffusion Model
IUPAC	International Union of Pure and Applied Chemistry
LDF	Linear Driving Force (model)
lmh	Liters per Meter Squared per Hour ($L/m^2/h$)
MCL	Maximum Contaminant Level
MDL	Minimum Detection Level
MF	Microfiltration
MV	Molar Volume

MW	Molecular Weight
NOM	Natural Organic Matter
N/A	Not Applicable
PAC	Powdered Activated Carbon
PAC/UF	Powdered Activated Carbon/Ultrafiltration
PAC/MF	Powdered Activated Carbon/Microfiltration
PVDF	Polyvinylidene Difluoride
S-PAC	Superfine Powdered Activated Carbon
SDBS	Sodium Dodecyl Benzene Sulfonate
SOC	Synthetic Organic Chemical
SRNOM	Suwannee River Natural Organic Matter
SVF	Specific Volume Filtered
UF	Ultrafiltration
USEPA	United States Environmental Protection Agency
UV/Vis	Ultraviolet/Visible (spectroscopy)
WC 800	Watercarb 800

Symbols

V_f	Filtered Volume through the Membrane
M_c	Carbon Mass
V_b	Bed Volume
Q	Volume Flow Rate
V_R	Fix-bed Volume

R_m	Membrane Resistance
R_c	Resistance Caused by Coating
ΔP	Transmembrane Pressure
J_o	Water Flux
μ	Water Viscosity

Chapter 1 INTRODUCTION

As the development of contaminant studies continues, the transport pathways of contaminants are understood better in the environment. These contaminants exist in water bodies, the atmosphere, and soil through global cycling. Thus, humans contact anthropogenic chemicals by using surface water and ground water. A national scale study revealed the presence of herbicides, steroids, flame retardants, pharmaceuticals, and plasticizers in drinking water sources (1).

Numerous data indicate that contaminants in drinking water have exceeded maximum contaminant levels (MCLs) set by the EPA (2). For instance, atrazine, a widely used herbicide that can cause cardiovascular system diseases or reproductive difficulties, has exceeded its MCL of 3 $\mu\text{g/L}$ at a Midwestern treatment plant on one or more occasions (3). As detection methods improve, the types of contaminants found in water will increase. Some contaminants may damage human health at concentrations lower than the detection limit. Therefore, it is essential to continue finding technical improvements for water treatment processes.

Natural organic matter (NOM) is also an important concern when treating drinking water because of its health effects and disinfection by-product (DBP). The merging membrane-activated carbon technology is widely used in drinking water treatment since it is effective at removing NOM and synthetic organic chemicals (SOCs) (4), and reducing the flux decline caused by NOM. The reduction of flux will decrease the efficiency of the membrane, therefore, minimizing fouling is vital in water treatment processes.

Powered activated carbon (PAC) has been studied in the project because of its large adsorption capacity. However, it became apparent that it was more important to study superfine powdered activated carbon (S-PAC) because of its higher adsorption capacity for both SOCs and NOM. Microfiltration membranes have also been selected due to their efficient particle removal. Different types of carbon (both PAC and S-PAC) and various environmental conditions were studied to the mechanisms of NOM competition with contaminant. The adsorption mechanisms of SOCs and NOM in S-PAC/membrane system were discussed. The project focused on the aggregation of activated carbons, various techniques of process, the effects of NOM concentration, solution pH, and how the flux varies with different parameters.

Chapter 2 BACKGROUND

2.1 Activated carbon

2.1.1 Origin and Production

According to the definition of the International Union of Pure and Applied Chemistry (IUPAC), activated carbon is “a porous carbon material, a char which has been subjected to reaction with gases, sometimes with the addition of chemicals before, during, or after carbonization to increase its adsorptive properties” (5). Carbonization is “a process by which solid residues with increasing content of the element carbon are formed from organic material usually by pyrolysis in an inert atmosphere” (5). In industrial practice, porous adsorbents are usually “activated” by treating them in high-temperature steam or gases with or without an oxidizing compound, which opens the carbon matrix and leads to micro and macro pores (6). The oxidizing compounds, such as potassium hydroxide and zinc chloride, act as the agents in chemical activation.

Normally activated carbon is prepared from coal, wood, and coconut shell (7, 8), but due to its high cost, cheaper sources like fly ash, silica gel, wool wastes, blast furnace sludge, and clay materials are of recent interest (8).

2.1.2 Applications

Adsorption processes are effective for the removal of colors, odors, and organic and inorganic pollutants from industrial processes or waste effluents. The main use of activated carbon in the United States is drinking water treatment (9). Granular activated carbon (GAC) and powdered activated carbon (PAC) are two typical types of activated carbon which are widely used, both having excellent adsorption capability, but varying in

particle size (6). Typically, the size of GAC particles varies between 200 and 1000 μm , and the size of PAC is from 20 to 200 μm .

2.1.3 Factors Influencing Adsorption

The effectiveness of activated carbon is influenced by various factors such as surface chemistry, pore structure, and particle size. The conditions of adsorbents and environmental solutions are also very important in the adsorption mechanisms. The summary of influencing factors is shown in Table 2.1.

Table 2.1 Factors Influencing Adsorption on Activated Carbon (9)

<u>Adsorbent Characteristics</u>	<u>Adsorbate Characteristics</u>	<u>Solution Characteristics</u>
<ul style="list-style-type: none"> ○ Porosity (interparticle and intraparticle) ○ Surface chemistry ○ Surface area ○ Particle size ○ Pore size distribution 	<ul style="list-style-type: none"> ○ Dimensions and molar volume ○ Polarity ○ Concentration ○ pK_a 	<ul style="list-style-type: none"> ○ pH ○ Water hardness ○ Temperature ○ Ionic strength ○ Competing species (i.e. organic matter)

The pore size distribution of activated carbon is a vital factor that affects the adsorption capacity. There are three pore sizes typically defined: macropores, which have diameters greater than 50 nm; mesopores, ranging from 2 nm to 50 nm; and micropores, which are less than 2 nm (10). Since the physical interactions of adsorption mainly depend on size distribution, if the size of the adsorbate is larger than the carbon pores, the target molecules are not well adsorbed by activated carbon. It is important because when small molecular weight SOCs and macromolecules such as NOM both exist in the system, the SOCs will be adsorbed better than macromolecules because of their size. However, NOM will adsorb to some degree and can hinder diffusion by pore blocking. Also, according to the conclusion of Karanfil and Kilduff (11), another physical interaction is microporosity. When other conditions are the same, and assuming the

adsorbent and adsorbate are chemically compatible, micropores have greater sorption energy because the limited space allows several potential adsorption points to overlap their forces.

The surface properties can also determine the adsorption through the existence of the surface functional groups. Normally we use zeta potential to quantify the electrical potential of the surface and interpret the results as changes of surface structures. Several possible types of functional groups are depicted in Figure 2.1 Examples of oxygen and nitrogen-containing functional groups on an activated carbon surface. Adapted from references (9) and (10).. Even though carbonaceous materials mainly hydrophobic, the hydrophilic character can be enhanced by attaching oxygen atoms to the surface, which will lead to the adsorption of water molecules. According to the research of Müller and Gubbins (12), the formation of water molecules are three-dimensional clusters centered on the active sites of the surface instead of as a monolayer. Karanfil and Kilduff (11) also found that the acidic groups reduce the adsorption of hydrophobic SOCs, accompanied by the polarity increase on the surface.

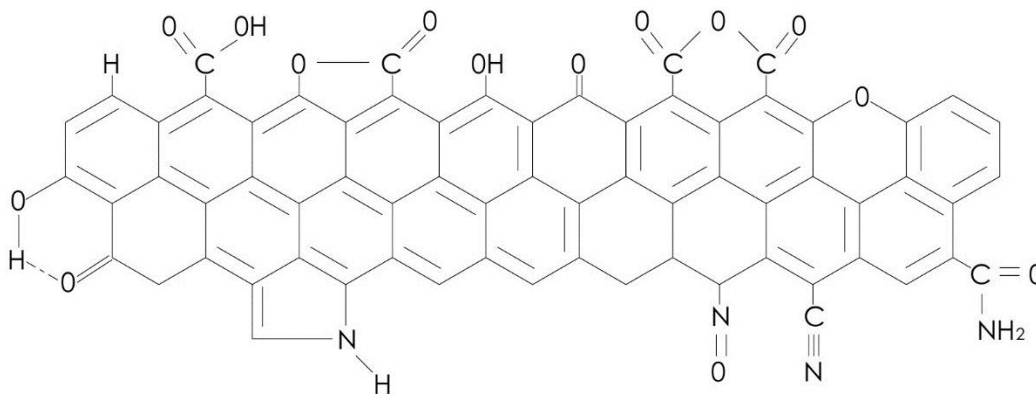


Figure 2.1 Examples of oxygen and nitrogen-containing functional groups on an activated carbon surface. Adapted from references (9) and (10).

Chemical studies indicate that numerous mineral ions--mostly calcium, sulfate and phosphate--occur in PAC samples (13). Changing the properties and number of the functional groups can be achieved through chemical/physical process. For instance, thermal treatment will decrease acidic groups and increase the electrokinetic potential (13). Other methods, including chemical oxidation and grafting of polymers, can also meet the goal.

Another important factor is contaminant concentration. The adsorption capacity at different concentrations can be concluded from the isotherm for the contaminant of interest. The adsorption capacity increases as concentration increases. However, in the small range of the concentration, the effect stated above may not be noticeable since adsorption capacity is essentially constant at relatively higher concentrations.

In addition to the carbon properties and contaminant concentration, the characteristics of the solution are also considerable for adsorption capacity. The pH value of the solution is one factor. Semmens et al. (14) pointed out that the adsorption of SOCs on GAC improved when the pH was low. Most of characteristics of the solution are related to the presence of other species, such as NOM in the solution. NOM can compete with the small-molecule SOCs during adsorption and block the carbon pores due to its large size. Some scholars found that the extent of decrease in adsorption capacity is dependent on the relative initial concentration of SOC compared to NOM (15, 16). This kind of initial effect is particularly important, especially when the NOM concentration is 3-6 orders of magnitude compared to SOC. Besides the concentration, other parameters like molecular size distribution and chemical composition also affect the competition. The most severe competition occurs when the sizes of NOM and SOC are similar and are

adsorbed concurrently. If the NOM has much larger sizes than contaminants, the competition will decrease (17, 18). However, if the NOM is preloaded onto the activated carbon, the adsorption of contaminant will decrease (17). It was found that if there are only small micropores on the carbon with little NOM competing with the SOCs, the competition is low. In contrast, if larger micropores are dominant with higher levels of NOM, the reduction of SOC adsorption is more obvious (19). The pore size distribution of the carbon not only influences the contaminant adsorption, it is also related to the competition of NOM and contaminants. Li et al. (20) reported that the best adsorption capacity of NOM is when the size of pores is around 15 to 50 Å.

2.2 Superfine Powdered Activated Carbon

Superfine powdered activated carbon (S-PAC) is activated carbon which has a finer particle size than PAC. It is usually produced by grinding PAC in a wet mill. Previous work showed that decreasing the carbon particle size and creating S-PAC removed phenanthrene and atrazine better than adsorbents with larger particle size in the presence of competitive adsorbents like natural organic matter (NOM). S-PAC typically has an average particle size of less than 1 µm, and the size of PAC is as large as 200 µm. According to the previous studies (21), the adsorption kinetics are faster when comparing S-PAC to PAC. Matsui et al. (22) pointed out that the adsorption capacity of S-PAC for geosmin compared to the adsorption capacity of PAC did not show a big difference; however, the kinetics of S-PAC for uptake of geosmin are faster than those of PAC. Also, the removal increased when particle size decreased to about 1 µm, although further decreasing does not cause a change in removal capacity. Another study showed the

dominant removal of large size NOM on S-PAC when compared to the adsorption on PAC. This kind of NOM does not compete with the adsorption of SOCs (23).

2.3 Natural Organic Matter

NOM is present in all natural water from degradation of terrestrial biomass which leaches from soil into a water source. Water treatment facilities target the removal of NOM because they are precursors to DBPs, which form as a result of chlorination. The reactions between dissolved organic matter (DOM) and oxidants or disinfectants such as chlorine can lead to the formation of DBPs. Since recognizing the severe health issues that DBPs caused, United States Environmental Protection Agency (USEPA) has imposed stringent regulations under the Disinfectants/Disinfection Byproducts Rule (D/DBP Rule) (24). NOM is a heterogeneous mixture with miscellaneous origins (inorganic and organic), sources (terrestrial, vegetative debris, and autochthonous input such as algae), and properties (including particulate and soluble). Normally, the molecular weight of NOM molecules is large (at least 2000). NOM also includes various functional groups such as phenolic, hydroxyl, carbonyl groups, and carboxylic acid. DOM is the most important component in considering membrane fouling since the DOM can cause irreversible fouling during filtration. Commonly, it is comprised of humic substances, poly-saccharides, amino acids, proteins, fatty acids, phenols, carboxylic acids, quinines, lignins, carbohydrates, alcohols, resins, and inorganic compounds such as silica, alumino-silicates, iron, aluminium, suspended solids and microorganisms (bacteria and fungi) (25). The hydrophobic part of NOM is around 50% based on dissolved organic

carbon (DOC) measurements, while other parts are hydrophilic and transphilic. The description of the distribution is presented in Figure 2.2.

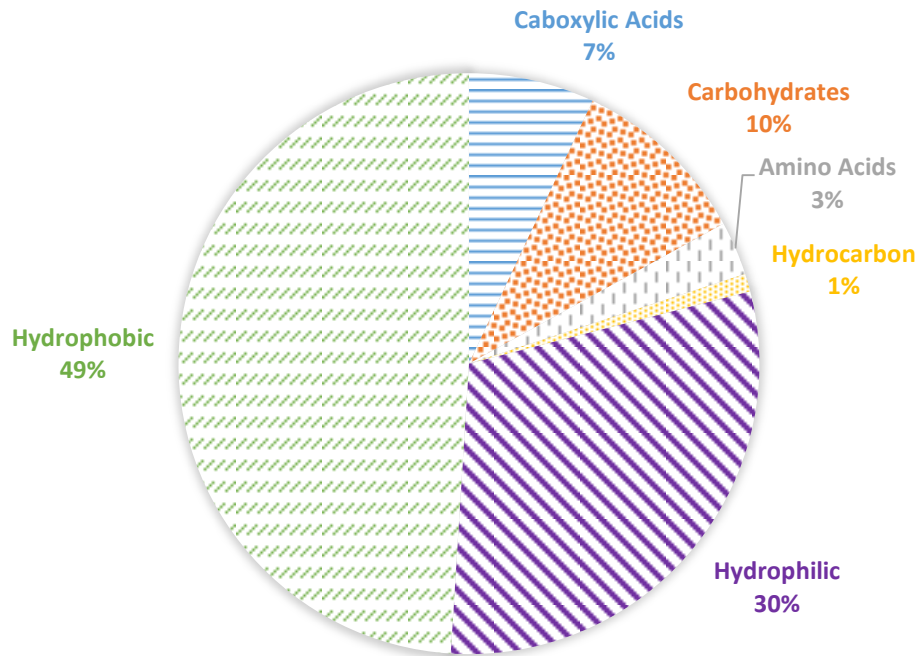


Figure 2.2 Fraction of NOM in surface water based on DOC (26).

The humic substances are the predominant components in NOM which are divided into three parts: humic acid (HA), fulvic acids (FA), and humin. HA and FA (Figure 2.3 and 2.4) are anionic polyelectrolytes with negatively charged carboxylic acid (COO^-), methoxyl carbonyls ($\text{C}=\text{O}$) and phenolic (O^-) groups. HA is more soluble in a higher pH solution and FA can be dissolved at any pH (27). In contrast, humin is not soluble at any pH. The properties of HA, FA, and humin are summarized in

Table 2.2.

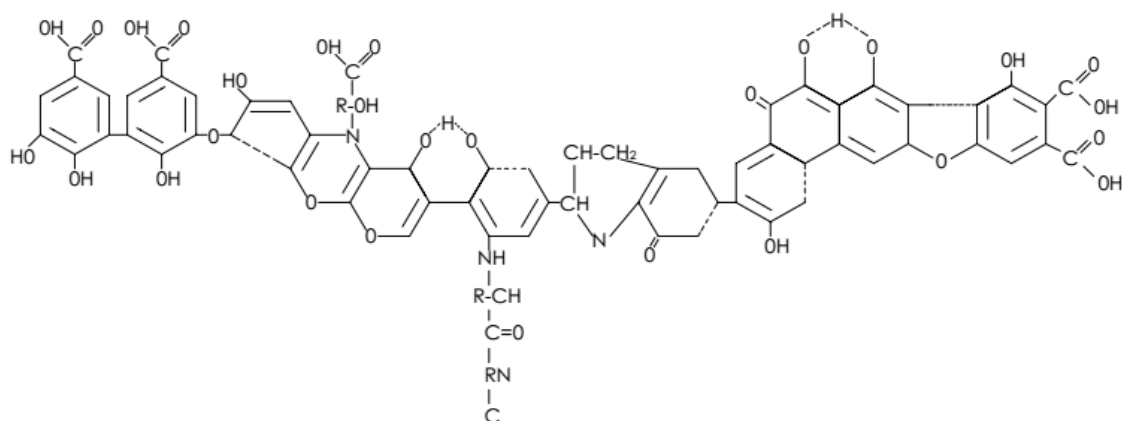


Figure 2.3 Schematic of humic acid model structure (25).

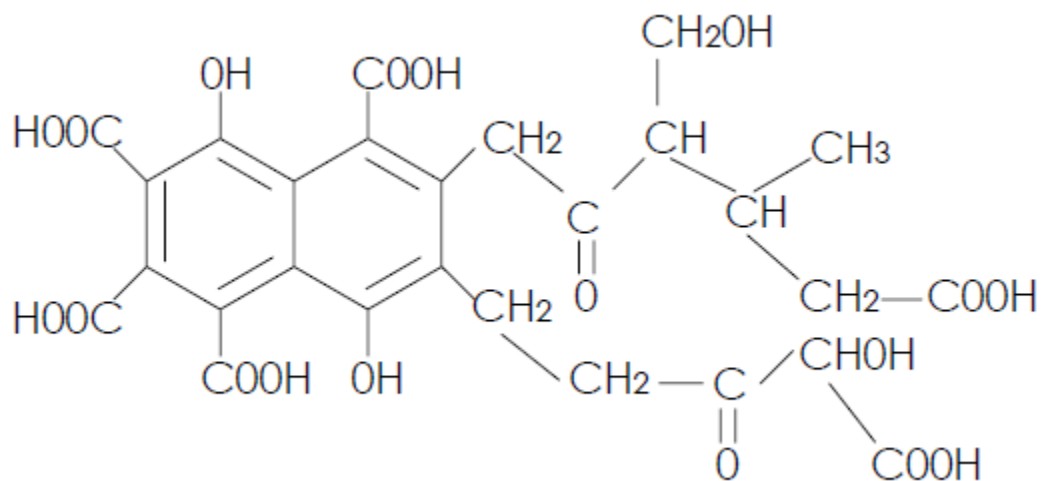




Figure 2.4 Schematic of fulvic acid model structure (25).

Table 2.2 Physical and chemical characteristics of humic substances (28).

	Fulvic acid		Humic acid		Humin
Color	Light Yellow	Yellow Brown	Dark Brown	Grey Black	Black
Polymerization	Increase in degree of polymerization 				
Molecular weight	2000	Increase in MW 300,000 and above			
Carbon content	45%	Increase in carbon content			62%
Oxygen content	48%	Decrease in oxygen content			30%
Exchange acidity	1400%	Decrease in exchange acidity			500%
Solubility	Decrease in degree of solubility 				

In natural water systems, the types of organic components of NOM may vary depending on the season (29), for instance, rainfall, snowmelt runoff, floods or droughts. Besides the quantity, the quality of NOM also changes. Some research showed that several important characteristics of NOM such as specific UV absorbance (SUVA) have been increasing (30). The change of NOM should be noticed since it would affect the choice of treatment process.

2.4 Adsorbent/Membrane Systems

As a hybrid membrane process, PAC/UF (powdered activated carbon adsorption/ultrafiltration) has been developed for controlling pesticides, taste and odor compounds, and disinfection by-products in drinking water treatment. Its main advantage is the combination of the ability of the PAC to adsorb organics, such as dissolved toxins, and the ability of UF membrane to remove particles, such as cyanobacteria, effectively. Considering the capital cost and flexibility for implementation improves, microfiltration (MF) and UF systems are more and more important in water treatment. More than a

hundred membrane treatment systems were installed in 2000 and this trend of installation is likely to continue (31). Another advantage of the hybrid system is the requirement of a small spatial footprint and low energy. Compared to reverse osmosis, which requires a pressure of 800-1000 psi, the advantage of PAC/UF is lower pressure required, thus saving energy. The applied pressure of PAC/UF is about 15 psi (31).

Furthermore, PAC can form a layer on the membrane during operation. PAC particles can accumulate on the membrane and form a layer (32). The PAC particles will rapidly accumulate on the membrane to form a layer which helps to prevent foulants from reaching the membrane. Additional research has demonstrated that in cross-flow filtration, the layer reaches a maximum thickness, after which PAC deposition equals removal due to the fluid flow (33). To remove foulants from the system and regenerate PAC, backwashing is needed every 30-90 minutes (34). Chlorine may be added during backwashing to prevent bacterial growth on the membrane (35). However, chlorine may decrease adsorption capabilities by oxidizing the carbon surface.

A carbon coating system involves the carbon being added directly before the membrane filtration without any stirring. The advantage of the coating technique is saving energy and construction space compared to the conventional PAC/UF. The setup does not need the stirring equipment to stir the adsorbent and water in the tank, thus saving energy. Also, without build the stirred tank can eliminate the space when set the whole PAC/UF system.

Carbon layer is considered a factor that influences membrane fouling. However, PAC particles are often large enough to prevent the flux deduction (33). In fact, the observation in some research shows that a PAC coated membrane prevents flux decline

to some degree, since PAC can adsorb some foulants (36-37). It is also a key advantage of the PAC coating technique. However, some literature reported the opposite finding: the membrane may be fouled by PAC (38). Lin et al (39) also reported that the presence of PAC resulted in more severe flux decline in the PAC/UF membrane. Previous research (40) also showed the differences in carbon adsorption between a batch PAC test and a continuous PAC/UF experiment. In all, one important consideration for the PAC/UF system is ensuring the compatibility of the adsorbent and membrane. When it comes to S-PAC, some research showed that S-PAC coating would lead to flux decline with hollow-fiber microfiltration membranes (41). Since the particle size of S-PAC is smaller than that of PAC, the increasing fouling caused by S-PAC is reasonable. Nevertheless, S-PAC coating technique was proved to have better atrazine adsorption kinetics compared with PAC on a lab scale, and have the effect of preventing biopolymer foulants (42).

Many factors like backwashing frequency, reactor size and configuration, filtration mode (dead-end versus cross-flow) and dosing procedure (step input versus phase input) can determine the adsorption performance of PAC/UF systems (43-44). The way that a PAC is added to a system could also affect the removal efficiency of organic matter and the required dosage of PAC. Lee et al. (45) showed that the removal efficiency of organic matter is enhanced and the carbon usage rate is decreased when mixing is complete and there is a longer detention time of the PAC. Other factors such as the point of PAC addition and the size and dosage of PAC also have an effect on the performance of the PAC-UF system. The location of the PAC addition, which is associated with the contact time between the PAC and the organic matter, can influence the result of the treated water. The contact time is prolonged and the NOM removal is improved when a separate

adsorption reactor is employed. Juang et al. (46) pointed out that the adsorption was rapid when using fine PAC (size <48 μm) and became slower with increasing PAC particle size, especially for the adsorption of the larger molecule sodium dodecyl benzene sulfonate (SDBS). Moreover, the characteristics of the carbon and the membrane can also affect the system performance. The adsorption rate will be faster when the PAC particles are smaller, and the amount of PAC particles required to achieve the same efficiency is reduced (47). Also, pH can affect the organics removal, which was lower at pH 6.5 than at pH 8.7 in PAC/UF processes (48).

Even the PAC/UF system is proved to eliminate the fouling in previous studies, the membrane fouling is still a big concern since NOM exists in the natural water systems. Generally, more severe membrane fouling caused by NOM occurs at a low pH, high ionic strength, and in the presence of divalent cations (49-56). This could be explained by the changes of intra- and intermolecular electrostatic gradients of the functional groups (COO^- and COOH). Buffering or shielding the charge of these functional groups can be eliminated by increasing the ionic concentration. This condition thus urges the aggregation of NOM and appears to have a higher molecular weight and surface area. Compared to monovalent cations, divalent cations were the main reason for fouling of membranes through complex action (57). Also, calcium ions can cause greater flux decline than magnesium ions do. This is due to the intermolecular bridging formed among NOM molecules through calcium ions. Magnesium ions can neutralize the negative charge of functional groups on NOM that leads to more compact structure. The impacts of divalent cations are mainly reflected in two aspects. One is that the presence of divalent cations (especially calcium ions) reduces the humic acid solubility. Another is

eliminating the negative charge effect of the functional group or bridging the negative membrane surface with the negative functional groups (26). Increasing the pH causes the ionization of the carboxyl groups, which improves the intramolecular repulsion and solubility. At low pH conditions, carboxyl groups of NOM are protonated and form large complexes which are less soluble. In contrast, Costa et al. (58) did an experiment with an ultrafiltration membrane and concluded that flux decline related to colloidal NOM was independent of pH. Molecular weight is another factor that affects fouling. The larger apparent molecular weight exhibited by NOM, the greater the flux decline and better permeate quality (59).

Cho et al. (60) concluded that the factors affecting the NOM-membrane interactions include properties of NOM (bulk NOM concentration, humic/non-humic fraction, molecular weight distribution, charge), properties of membrane (physical structure, surface/pore charge, hydrophobicity), properties of solutions such as pH and ionic strength, and operating conditions. Also, in adsorbent/membrane systems, carbon properties and the ways carbon is added are other factors that influence fouling. In previous research (61), the fouling potential of various water types was (from most potential to least potential): hydrophilic neutral>hydrophobic acids>transphilic acids>hydrophilic charged. Membrane properties can also affect the fouling. The degree of fouling on hydrophobic membranes is greater than on hydrophilic membranes. Compared to UF, MF leads to more flux decline during filtration (62). Different driving forces of fouling may be the reason. For MF, pore blockage by large hydrophilic molecules and/or organic colloids may be the main force of fouling. For UF, a gel layer may form and cover the membrane during the filtration, which causes the fouling. Two

mechanisms of NOM fouling were identified (58). In early stages, pore blocking was the main mechanism. For longer filtration, there was a transition in the mechanism from pore blocking to cake formation. Organic matter was found to be packed under the inorganic fouling layer, forming a gel-like organic matrix (49). The morphological analyses (62) showed membrane roughness may be a vital factor of fouling because of interaction between molecules and membrane surface.

Pressure is also an important factor affected fouling. Some research (63) showed that pressure would influence the initial flux and the results of convective transport of foulants towards the membrane surface. Severe fouling was caused by higher permeate flux because of higher permeate drag and more compressed foulant layers (49, 60). In conclusion, even if the higher permeate flux at the beginning is an advantage, the following rapid flux decline due to severe fouling may decrease the advantage.

Chapter 3 RESEARCH OBJECTIVES

This project evaluated the competition of NOM and SOCs in the activated carbon/microfiltration system. Specifically, the objectives were as follows:

- (1) ***Compare membrane flux decline with PAC and S-PAC, including aggregation effects.*** Various parameters were tested, such as the carbon type, carbon amount, and methods of carbon addition, sonication type, sonication time, and power. These were used to develop consistent experimental methods for further work, and also to give insight into the behavior and interactions of carbon with membranes.
- (2) ***Evaluate contaminant removal for PAC and S-PAC in deionized water.*** Different contaminants and concentrations were used to measure the adsorption capacity and contaminant behavior with no background NOM.
- (3) ***Measure contaminant removal when NOM is present.*** Two types of NOM, natural Edisto River water and Suwannee River NOM (SRNOM) were used to test for competitive adsorption. The differences in competitive adsorption behavior between PAC and S-PAC were also discussed.
- (4) ***Evaluate flux decline in the presence of NOM.*** The flux change in the presence of NOM was evaluated which supported the mechanistic studies of competition between SOCs and NOM. As mentioned before, since activated carbon and NOM can both cause fouling, the main driving force of the fouling was explored under this objective.

(5) *Determine the effects of solution pH and NOM concentration.* Various pH and NOM concentrations were used in filtration experiments to help elucidate the NOM competition mechanisms as well as the membrane fouling mechanisms.

Chapter 4 MATERIALS AND METHODS

4.1 Adsorbents

Three types of carbon were used in this project: coal based WPH, Norit 20B, and Watercarb 800. S-PAC was produced from the corresponding PAC in a wet-mill micro-grinding process at Netzsch Premier Technologies. WPH PAC and S-PAC were used in the method development experiments to understand the aggregation of the carbon. The NOM competition experiments used Norit 20B and WC 800. WPH, Norit 20B and WC 800 were purchased from Calgon Carbon Corporation, Norit Americas Inc. and Standard Carbon LLC, respectively. All adsorbents were weighed on a microgram balance (Mettler Toledo MX5) in dry powder form and then prepared as 2000 mg/L stock solution with distilled deionized water (DDI) before use.

4.1.1 Properties of adsorbents

The properties of Norit 20B and WC 800 are shown in Table 4.1. Comparing the pore sizes of the two carbon types, Norit 20B has relatively large pore size. Meso-pores take the biggest ratio (58.5%) of the carbon pores which is in the size range from 2 to 50 nm. However, with WC 800, micro-pores dominate, at 47.3%. Thus, from the analysis of the carbon pore size, NOM may block the WC 800 more easily than Norit 20B since the pores are smaller. Both adsorbents are coal based carbons.

Table 4.1 Properties of the activated carbon materials investigated.

Commercial Name of the Carbon		WPH	Norit 20B	WC 800	
Carbon Type		Coal Based	Coal Based	Coal Based	
Iodine Number (mg/g)		N/A	800 min	800 min	
Surface Area BET (m ² /g)		900	1748	713	
Total Pore Volume (cm ³ /g)		0.2770	1.4225	0.4887	
Pore size Distribution	Micro	(<2 nm)	0.26	0.33	0.23
	Meso	(2<x<50 nm)	0.02	0.83	0.15
	Macro	(>50 nm)	0.00	0.26	0.10
% Pore size Distribution	Micro	(%)	92.78	23.03	47.30
	Meso	(%)	7.22	58.49	31.62
	Macro	(%)	0.00	18.47	21.08
pH pzc		6.43	5.4	10.37	

Refer to Table 4.2, the average diameters for WPH PAC and S-PAC were obtained from Ellerie (64) which were 25 (\pm 14) μ m and 0.23 (\pm 0.02) μ m, respectively. According to the reports from Netzsch, for WC 800, the average diameter of PAC and S-PAC were 21 μ m and 0.20 μ m. The average diameter of Norit 20B PAC and S-PAC were 28 μ m and 0.43 μ m.

Table 4.2 Particle size of different carbon

	Average particle size (μ m)		
	WPH	Norit 20B	WC 800
PAC	25	28	21
S-PAC	0.23	0.43	0.20

4.2 Adsorbates

Two types of adsorbates were chosen to test the removal efficiency and NOM competition.

4.2.1 Atrazine

Atrazine, a member of the chloro-s-triazine class, was selected as the main example contaminant for these experiments. Figure 4.1 (a) shows the molecular structure of atrazine and Table 4.2 has the chemical and physical properties. Atrazine is an herbicide used extensively in agriculture (66). It adsorbs fairly well to activated carbon, a trait that may result in part from the aromatic structures and corresponding ability to undergo π - π interactions with adsorbents. Radiolabeled atrazine with carbon 14 was purchased from American Radiolabeled Chemicals, Inc., and used as a tracer in conjunction with non-labeled atrazine from Accustandard, to enable detection with a liquid scintillation counter (LSC). Radiolabeled stock solution was not diluted with the non-labeled atrazine. Instead, the feed solutions for individual filtrations were adjusted with the non-labeled atrazine in a certain ratio. Two batches of atrazine were used in this project. Both of them had the activity of 160 mCi/mmol. The concentration, 0.5mg/L, of radiolabeled stock solutions were prepared in ethanol, and aliquots are transferred to distilled deionized water (DDI) to make feed solutions. The feed solutions for individual filtrations were adjusted with the non-labeled atrazine in a 1:29 ratio (Appendix A). The detection limit was calculated as 0.07 ppb. NOM experiment from Section 5.2.1 to Section 5.2.5 were used the first batch of the atrazine. The minimum detection level (MDL) of the second batch was measured (Appendix B) and a new ratio of radiolabeled to non-radiolabeled was determined according to the MDL and was used in the experiment section, which was 1:300. The new radio-labeled atrazine was prepared with ethanol at 1.34 mg/L. Permeate atrazine concentrations were measured with an LSC (Tri-Carb B2910TR, PerkinElmer). Each LSC measurement vial contained 5 mL of sample

and 5 mL of liquid scintillation cocktail (UltimaGold XR). The count time was 15 minutes per sample.

4.2.2 Carbamazepine

Carbamazepine, an anti-epileptic drug, was chosen as the second trace compound. The molecular structure of carbamazepine is shown in Figure 4.1(b) and various chemical and physical properties are listed in Table 4.3. A stock solution was prepared to a concentration of 1000 ppm by adding 4mg carbamazepine (MP Biomedicals, LLC) in 5mL of methanol. Carbamazepine was detected at 210 nm by C18 5 μ m 4.6 X 150 reversed phase HPLC column; 50 percent methanol and 50 percent water were used as the mobile phase.

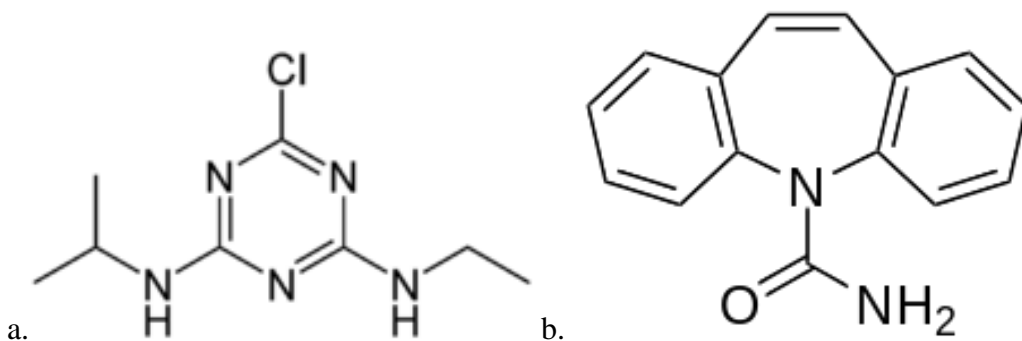


Figure 4.1 Molecular structures of atrazine (a) and carbamazepine (b).

Table 4.3 Adsorbate Properties

Compound	Atrazine	Carbamazepine
Chemical Formula	C ₈ H ₁₄ ClN ₅	C ₁₅ H ₁₂ N ₂ O
Dimensions (Å)	9.6×8.4×3 ^a	5.2×20.6×22.2 ^d
MW (g/mol)	215.7	236.3
Molecular Volume ^b (m ³ /kmol)	0.247	
pK _a	1.95 ^c	13.94
Solubility in Water (g/L)	0.03 ^e	0.02
log K _{ow}	2.75 ^e	8.19

^a Ref [59] ^b Estimated using Le Bas method . ^c Ref [65]

^e Ref [66] ^d Ref [67]

4.3 PAC/MF Experiments

The lab-scale dead-end MF setup, shown in Figure 4.2, consisted of an 800 mL pressure vessel (Millipore) that held the feed solution, a 10 mL capacity Amicon cell (Millipore) containing the MF membrane and mesh support material, glassware for permeate collection, and a balance connected to a computer to monitor the flux (Appendix C). The software used to measure the flux is Labview (National Instruments) (Appendix D). Pressure for the filtrations was supplied by a nitrogen tank connected to the pressure vessel. The membranes (Millipore VVLP) were hydrophilic Polyvinylidene fluoride (PVDF) with a pore size of 0.1 μm and diameter of 2.5 cm (2.1-cm active diameter when installed in the filtration cell). Membranes were soaked in DDI water overnight before use in filtrations. The pressure was fixed at 10 psi.

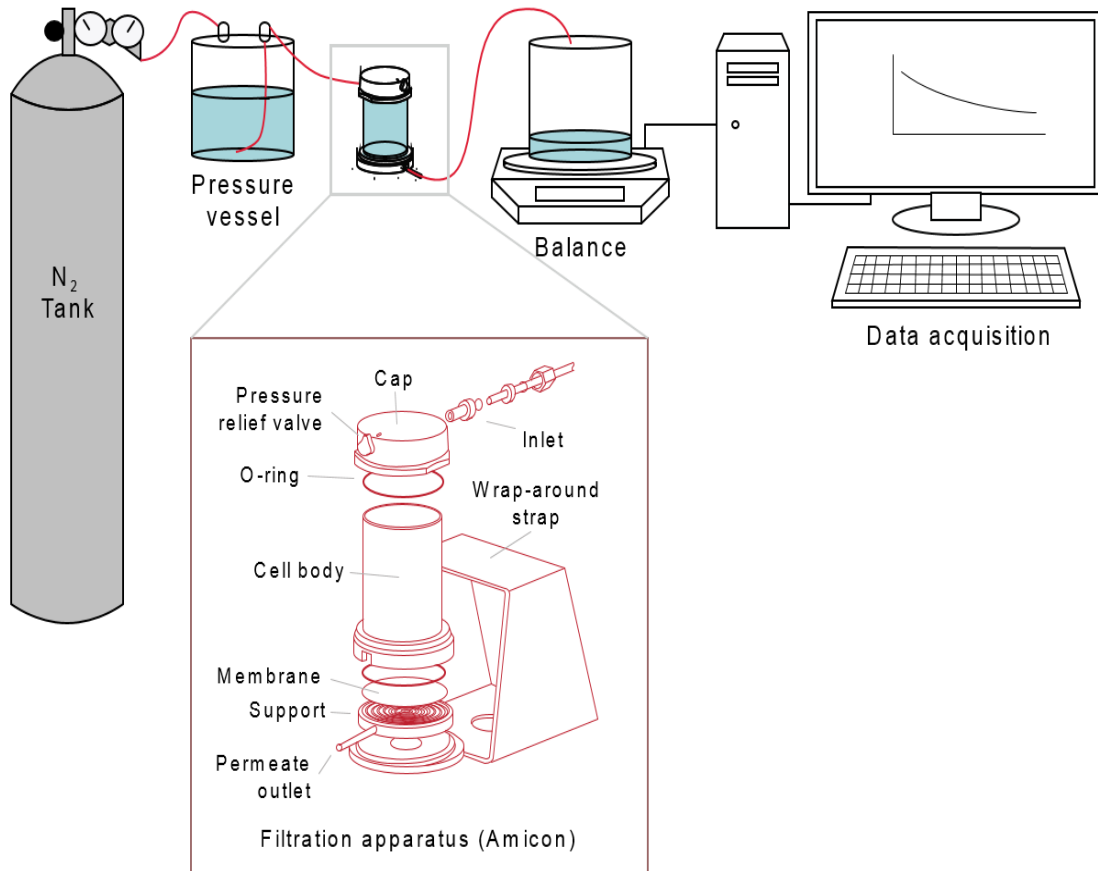


Figure 4.2 The bench-scale microfiltration setup (67).

4.3.1 Flux Decline Experiment

Several kinds of carbon including WPH PAC, WPH S-PAC, WC 800 PAC, WC 800 S-PAC, Norit 20B PAC, and Norit 20B S-PAC were used in the flux decline experiment. The first step was to determine the flux for the blank membrane, which was achieved with filtration of DDI water for 10 minutes. For the second step, a specified mass of adsorbent was added to the membrane cell, and the flux decline was determined without changing the pressure. Permeate samples were collected in glass beakers. Probe sonication and bath sonication were used to break the aggregation. A set of carbon

concentration and sonication time were tested. Also, membrane-coated test (added the carbon directly into Amicon cell) and stirred vessel test were done. During the stirred vessel experiment, a stir bar was added into the pressure vessel and a magnetic stir plate was put under the vessel.

4.3.1.1 Sonication

Two kinds of sonicators were applied in this project to disaggregate the carbon particles. Two kinds of sonicators, a probe sonicator (S-4000, Qsonica, LLC) and a bath sonicator (2510, Branson) were applied. Ultrasonic vibration can cause cavitation, the formation and violent collapse of microscopic bubbles. These bubbles will release tremendous energy in the cavitation field during collapse. Since the probe is directly contacted with the solution, the power will be stronger than a bath sonicator. To evaluate the effect of different aggregation states, or rather, different levels of disaggregation, the sonication time and power were varied before flux experiments.

4.3.2 NOM Experiments

Edisto River (South Carolina) water was used as one source of natural organic matter. The raw water had a 12 mg/L DOC value. We diluted the raw Edisto River water to 4 mg/L DOC with DDI water. Before experiments, the diluted Edisto River water was filtered by glass microfibre filters (Whatman) to remove the large suspended particles. The DOC was measured after filtration. The nominal pore size of the glass microfiltration filter was 0.15 μm .

Another source of NOM was Suwannee River NOM (SRNOM) (RO isolation) obtained from the International Humic Substances Society (Golden, Colorado). Stock

solutions (1 g/L) were prepared by dissolving the SRNOM in DDI water, adding a weak buffer (1 mM sodium bicarbonate) and adjusting the pH to 7 through the addition of hydrochloric acid, and/or sodium hydroxide. DOC was measured using a Shimadzu TOC-VCHS or TOC-LCHS high temperature combustion analyzer. DOC standards were prepared by diluting 1000 mg C/L potassium hydrogen phthalate solution in the range of 0.2-15 mg C/L. A calibration curve was taken before each measurement batch; details of the calibration curve procedures are shown in the Appendix E.

During membrane filtration experiments, permeate samples were collected in glass vials (20 mL) every 20 grams and analyzed with a UV/Vis spectrophotometer (Genesys 20) at 254 nm. A calibration curve between UV254 absorbance and NOM concentration was used to evaluate the NOM during filtration. Atrazine concentrations were determined from the same samples using the LSC methods reported above.

4.3.3 Calculation of Carbon Usage Rate

Carbon usage rate (CUR) determines the rate at which carbon will be exhausted and the frequencies of carbon replaced/regenerated (68). In drinking water treatment, the optimum parameters are typically selected after evaluating capital and operating costs, which are associated with use efficiency, such as CUR. In this project, CUR values were calculated using data from experiments with PAC and S-PAC. The calculation of CUR is expressed as:

$$\text{CUR} = \frac{V_f}{M_c} \quad (4.1)$$

In this equation, V_f represents the filtered volume through the membrane. M_c represents the carbon mass which can remove SOCs to a given level (usually 90% removal).

4.3.4 Empty Bed Contact Time and Bed Volume

Empty bed contact time (EBCT) is used to represent the length of time that liquid is in contact with the activated carbon bed. It is related to the removal kinetics since the shorter the contact time, the faster the adsorption kinetics must be. In this project, instead of a large bed depth, as found in most industrial carbon adsorbers, a very thin membrane coating of activated carbon was used, which results in a tiny EBCT.

In these experiments with an Amicon cell, EBCT is expressed as:

$$EBCT = \frac{V_b}{Q} \quad (4.2)$$

In the equation, V_b represents bed volume (L). Q represents the volume flow rate (L/min).

The number of bed volumes (BV) that pass through the filter can be calculated by:

$$BV = \frac{V_f}{V_R} \quad (4.3)$$

V_f is the filtered volume through the membrane (L), V_R is the fix-bed volume (L).

4.3.5 Membrane Resistance

Membrane resistance can be calculated by

$$R_m = \frac{\Delta P}{\mu J_o} \quad (4.4)$$

or by

$$R_m + R_c = \frac{\Delta P}{\mu J_o} \quad (4.5)$$

R_m is the membrane resistance and R_c is the resistance caused by coating. ΔP represents the transmembrane pressure. J_o is the water flux. μ is water viscosity. Equation 4.4 and 4.5 can be used to calculate the resistance due to the carbon coating to understand the coating mechanisms to some extent.

Chapter 5 RESULTS AND DISCUSSION

5.1 Flux Decline Experiments

5.1.1 Comparing flux decline between PAC and S-PAC

WPH PAC and WPH S-PAC were used in the flux decline experiments to understand how the carbon interacted with the membrane. A hydrophilic PVDF membrane with a pore size of 0.1 μm was used. Constant pressure (10 psi) filtrations consisting of two stages were run to determine the extent of membrane fouling by the adsorbents. The result is presented in Figure 5.1. The first data portion up to 15 minutes was the clean water flux, which is the first stage, and followed by the flux with added adsorbents, which is the second stage. Normalized flux is the flux with added adsorbate divided by the clean water flux.

To understand the coupon-to-coupon variability in membrane flux measurements the mean and standard deviation of twenty clean-water flux runs were evaluated. The mean was 2011 L/m²/h and the standard deviation was 216 L/m²/h. Clean-water flux in each experiment varies because of heterogeneities in polymer structure from coupon to coupon. Also, because the pressure was set with a manual dial and analog pressure gauge, there was some deviation around the 10 psi goal. A clean-water flux of 2000 \pm 200 L/m²/h was considered acceptable; all flux data were normalized to the clean-water flux of the coupon to minimize the effects of this natural variability on data interpretation.

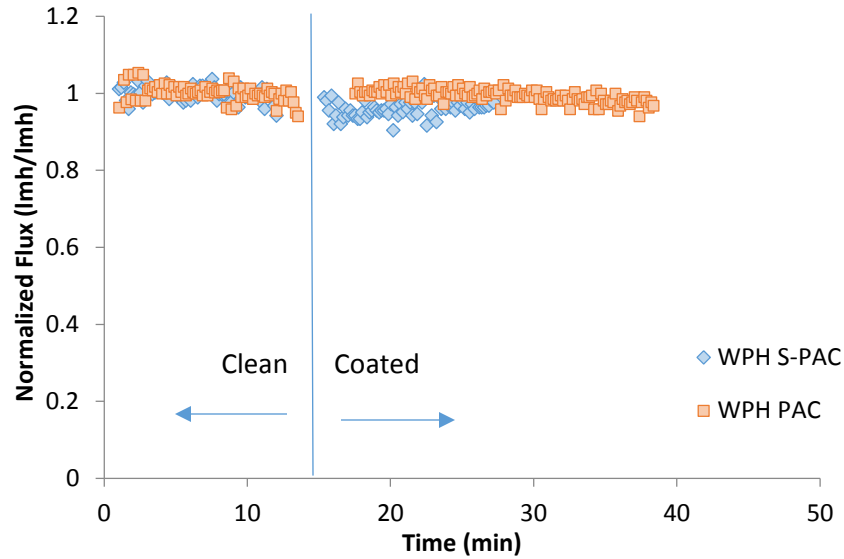


Figure 5.1 Flux data with WPH PAC and WPH S-PAC with the pressure of 10 psi. The membrane was coated with 3 mg carbon. The average DDI water flux in the WPH PAC experiment was 2212 lmh and that in the WPH S-PAC experiment was 2106 lmh.

From Figure 5.1, WPH PAC and WPH S-PAC (taken directly from the bottle in which they was stored) were confirmed not to cause flux decline on the 0.1 μm membrane. The flux before and after adding the carbon did not show a big difference. WPH PAC has an average particle size of 25 μm which is much larger than the membrane pore size, so pore blockage is minimal. However, S-PAC has a similar size with that of the membrane pores, which is 0.23 μm . It was hypothesized that in this case the particles of S-PAC aggregated to larger particles because of particle-particle interactions.

5.1.2 The effect of bath sonication

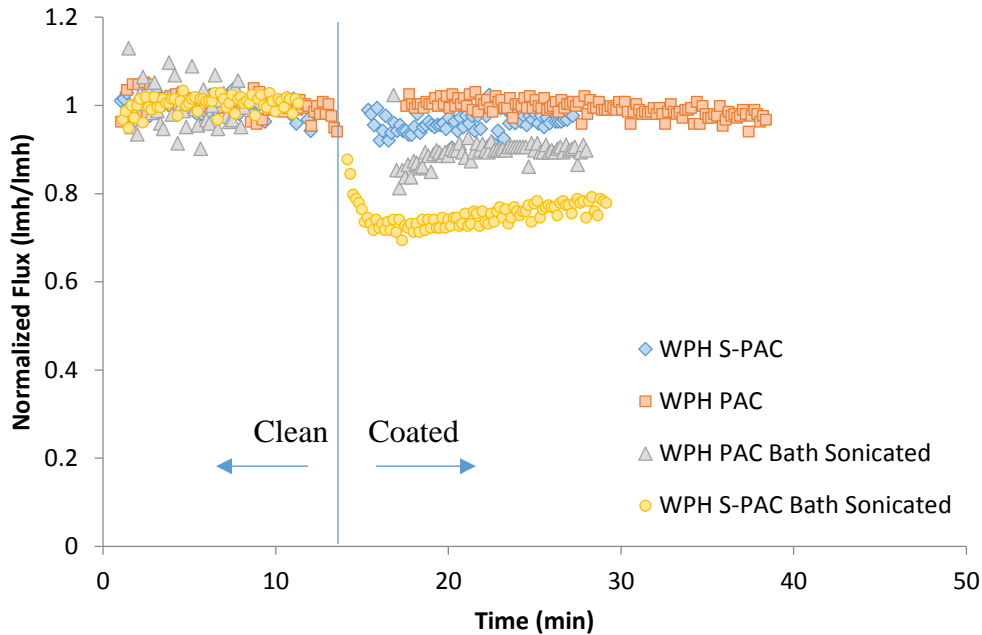


Figure 5.2 Flux data with WPH PAC and WPH S-PAC with and without bath sonication at the pressure of 10 psi. The membrane was coated with 3 mg carbon. The average DDI water fluxes were 2206, 2112, 2331, and 2015 lmh, respectively, for the experiments in the legend, top to bottom.

Since the carbon aggregated to larger particles, the benefit of the super-fine milling might not be realized unless disaggregation is implemented. A bath sonicator was first tested for its ability to disaggregate the particles. Figure 5.2 shows the comparison between carbon with and without bath sonication. Bath sonication was used in the stock solution of adsorbents just before (within 50 minutes of) the experimental run. As stated above, the WPH S-PAC had a particle size less than 1 μm , and the WPH PAC was 25 μm . However, when sonicating the carbon particles before an experiment, the sonicator can generate acoustic streaming and cavitation bubbles to provide force for particle isolation. Then the disaggregated fine particles of S-PAC can more easily block the membrane and cause fouling. The flux decline caused by S-PAC was about 30 percent.

For the PAC particles, although the bath sonicator may have caused some disaggregation the particles were still large enough to not cause much fouling.

5.1.3 Comparison of probe sonication and bath sonication

Probe sonication provided stronger power and energy as Section 4.3.1.1 described. To compare the effects of these two sonicators and set parameters for future experiments, data were collected as shown in Figure 5.3. Bath sonication was performed for 50 minutes and probe sonication was performed for 5 minutes at 50% power. Since the particle size of WPH PAC was larger than the membrane pores, the flux data were the same even when using the probe sonicator. For S-PAC, the probe sonicator disaggregated the carbon to a larger degree, which induced more severe membrane fouling; the flux decline caused by probe sonication on S-PAC was about fifty percent.

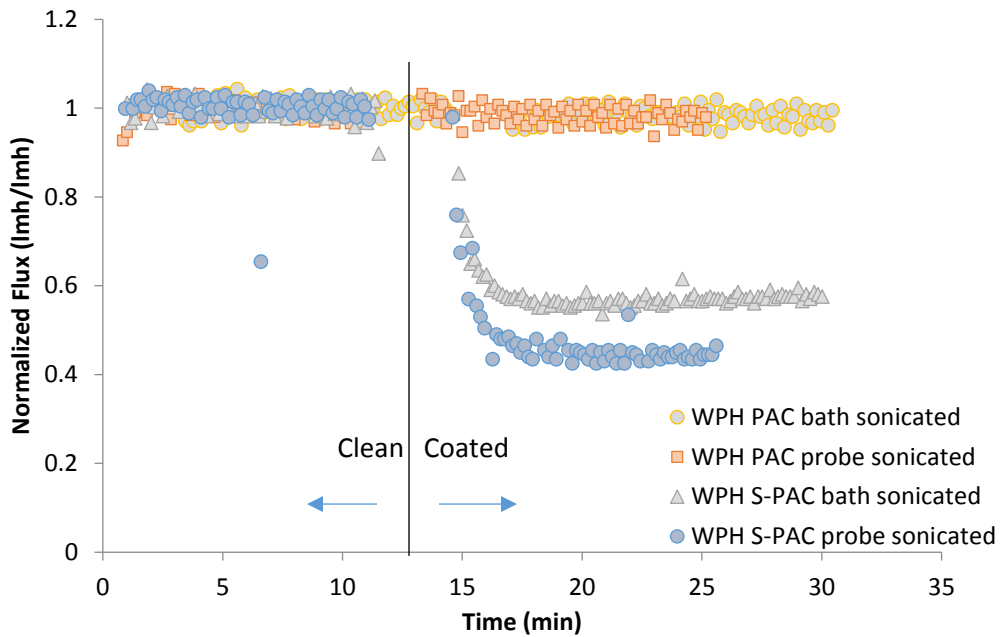


Figure 5.3 Flux data with WPH PAC and WPH S-PAC with bath sonication and probe sonication, separately, at the pressure of 10 psi. The membrane was coated 3 mg carbon. The average DDI water fluxes were 1897, 1985, 1910, and 1981 lmh, respectively.

5.1.4 The effect of sonication time on flux decline

To understand whether longer sonication times would lead to more complete disaggregation, different times of probe sonication were measured. The data are shown in Figure 5.4, all performed with 50% sonicator power. The flux decline did not show a large difference, even though the ten-minute flux was the lowest. Most of the flux data were overlapped. From the results, it was determined that the probe sonicator can provide large enough power that S-PAC particles was dispersed completely within a short period of time. With the carbon particles fully disaggregated, the flux decline caused by S-PAC reached 60 percent.

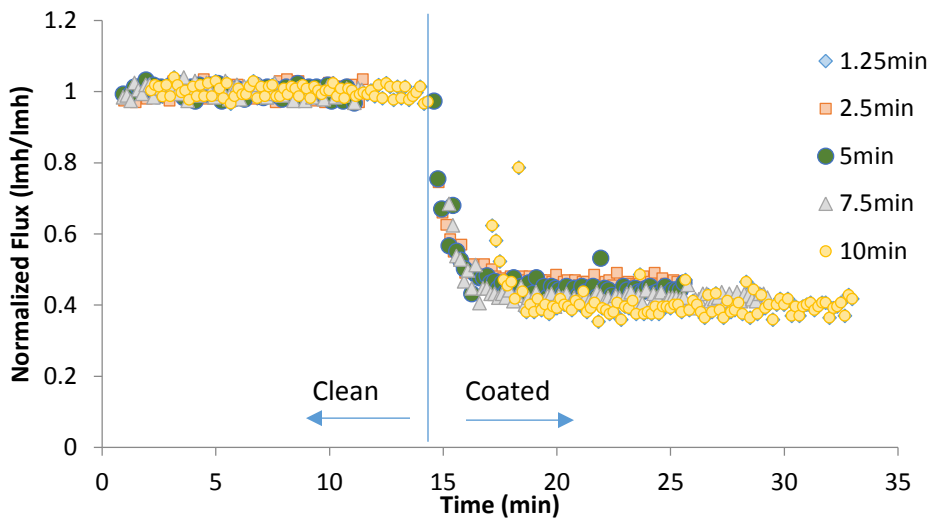


Figure 5.4 Flux data with WPH S-PAC with different time periods of probe sonication at the pressure of 10 psi. The membrane was coated with 3 mg carbon. The average DDI water fluxes were 1970, 2081, 1908, 2050, and 1970, respectively.

5.1.5 The effect of sonication power on the flux decline

Similar to the question of sonication time, sonication power was also a key parameter for S-PAC disaggregation. In another set of tests the time was set at 5 minutes while the power was varied. The results from this experiment are shown in Figure 5.5.

Disaggregation was most complete and caused the greatest flux decline when the power was 75%. The flux decline of 100 percent power and 50 percent power almost overlap. There were no large differences on the flux among these three power values; the minor decline of flux in 100% power compared to others may be caused by random variability. Since all power levels behaved similarly, the following experiments were set to use 50% power. Benefits to the lower power include less sample heating, less noise, and less wear and tear on the sonicator.

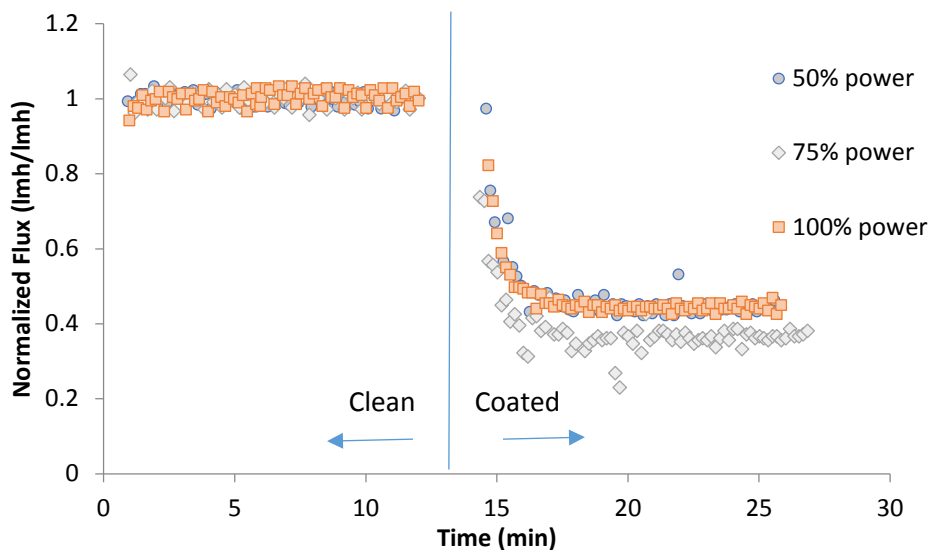


Figure 5.5 Flux data with WPH S-PAC with probe sonication at different power levels. Pressure was 10 psi. The membrane was coated with 3 mg carbon. The average DDI water fluxes were 2129, 2175, and 1908,lmh, respectively.

5.1.6 Comparison of flux decline with different adsorbents

Most of the experiments for flux decline were done using one carbon type. It was important to test other carbon type to see if the flux decline was consistent across types of carbon. Figure 5.6 shows the flux data with different types of S-PAC carbons. Norit 20B caused the least flux decline compared to the clean water, and WPH caused the most at nearly 50%. The observed behavior was consistent with the particle size of the carbons

(Table 4.2). The average diameter of Norit 20 B is about 0.43 μm , which is so much larger compared to membrane pores (0.1 μm). Since the large particles of Norit 20B S-PAC was more, the degree of fouling was smaller. The fouling was most severe with WPH, indicating that the distribution of particle sizes favored the less than 0.1 μm size. Norit 20B can lead to 10 percent flux decline and WC 800 can cause around fifty percent.

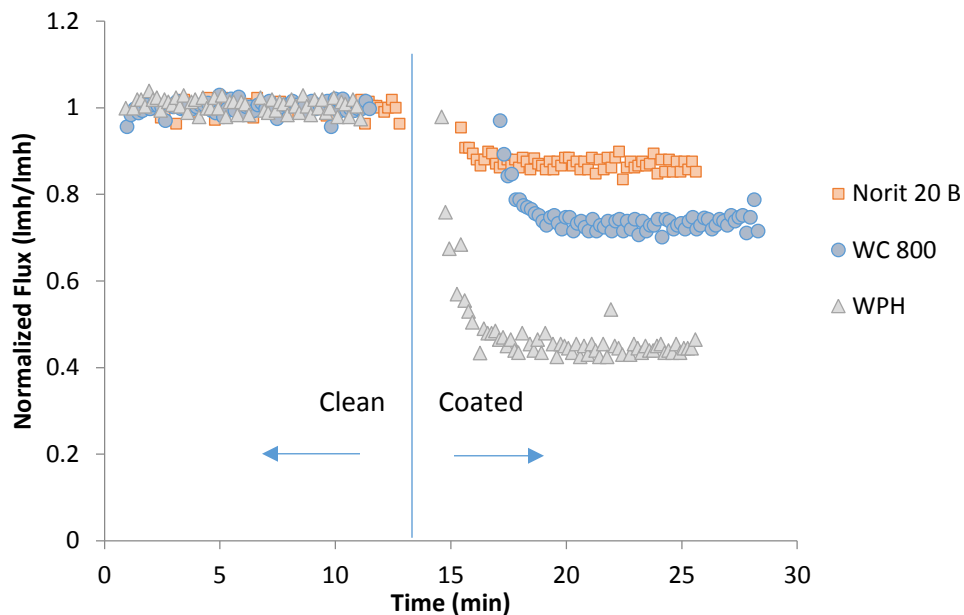


Figure 5.6 Flux data with various S-PAC type at the pressure of 10 psi. The membrane was coated 3mg carbon. Probe sonication at 50% power and 5 minutes was performed before using. The average DDI water flux is 2283 lmh at experiment with WC 800, 2257 lmh at experiment with Norit 20B, 1987 lmh at experiment with WPH.

5.1.7 Comparison of the effect of carbon addition method

It was important to determine whether there was a difference between adding carbon gradually over time or adding it all at once to form a fast coating. If there were a difference in the flux behavior, that could be a factor in designing an optimal process. The data from different carbon addition method experiments are shown in Figure 5.7. For PAC the two methods did not greatly influence the flux value. However, since the S-PAC

causes more obvious fouling, the flux data were more obviously different. As one would expect, immediate carbon addition to form a coating resulted in an immediate flux decline. The flux was reduced to 40 percent of the initial value and kept stable since no additional carbon was added.

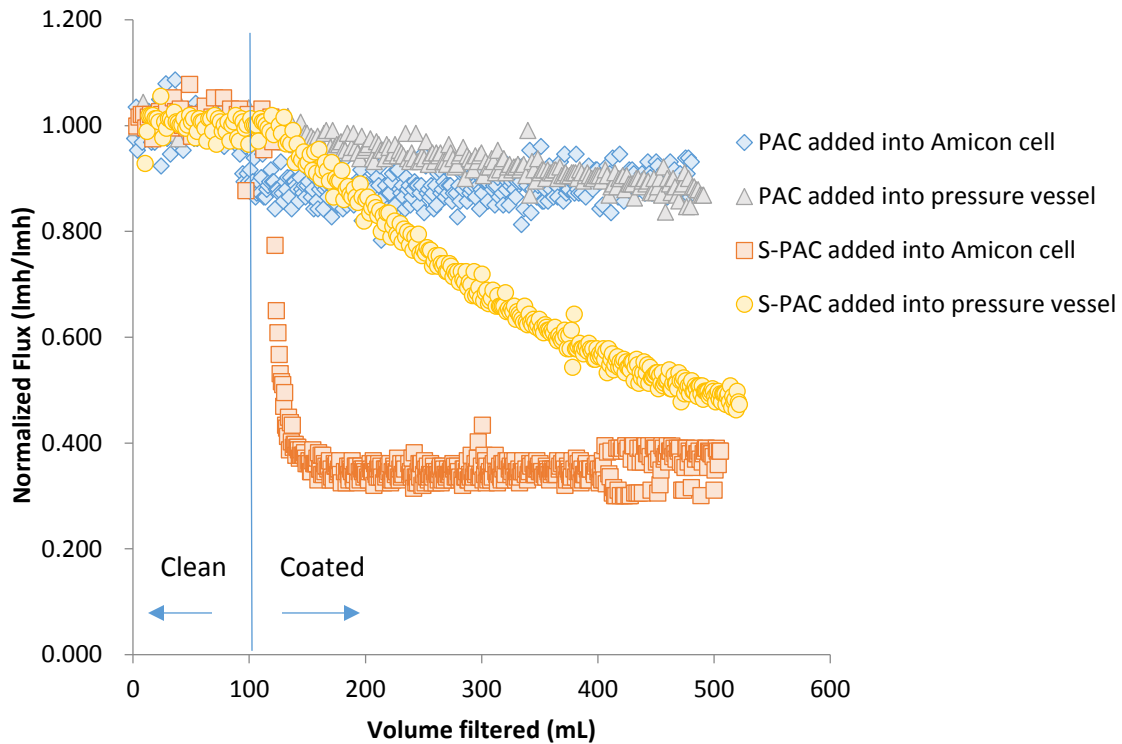


Figure 5.7 Flux data with WC 800 PAC and S-PAC added in Amicon cell and pressure vessel, separately, at the pressure of 10 psi. The carbon mass coated on the membrane was 3 mg. Probe sonication at 50% power and 5 minutes was performed before using. The feed solution contained methylene blue at 0.9 mg/L. The average DDI water flux was 1407 lmh for experiment with PAC in Amicon cell, 1952 lmh for experiment with PAC in pressure vessel, 2016 lmh for experiment with S-PAC in Amicon, and 1715 lmh for experiment with S-PAC in pressure vessel.

Compared to the coating method, the flux decline (Figure 5.7) was more gradual in the pressure vessel addition method since the solution with carbon was contacted with the membrane gradually. That result is to be expected, but it is interesting to consider whether the fouling was different on a per-mass-added basis. The flux data were plotted

versus the carbon mass in Figure 5.8. If the flux decline mechanism were the same between the coating technique and the pressure vessel (steady addition) technique, the flux should be the same when the mass of coated carbon is equal. If there were differences in deposition patterns or coating packing, the fluxes would vary. Figure 5.8 shows that the data were inconclusive; in one case the coating technique gave a larger flux and in another case the coating technique gave a smaller flux per carbon mass. This was potentially due to experimental variability and the small sample size used in the analysis; however, the analysis does show that there is no obvious and consistent difference between fluxes observed with the coating versus continuous addition methods. More experiments should be done to confirm this behavior.

Figure 5.8 shows the relationship between coated carbon mass and flux with different added carbon in pressure vessel. Since the addition of carbon is the same, ideally the mechanisms of carbon coating should be the same. However, there should be a loss of carbon when the carbon was moved from the pressure vessel to the Amicon cell. Carbon particles may stick to the walls of pressure vessel and tubing. This minor deviation may cause these flux curves to converge but not overlap completely. Besides, since the experiments were only done without repeating, the deviations due to the experiments are not certain. One feature to notice is that the curves of steady addition were not linear. The results indicated that the coating mechanisms may change during the experiments. At first, the particles can block the membrane pores which will cause severe fouling. After that, the S-PAC particles will form the cake layer which does not influence the fouling as much as the pore blocking.

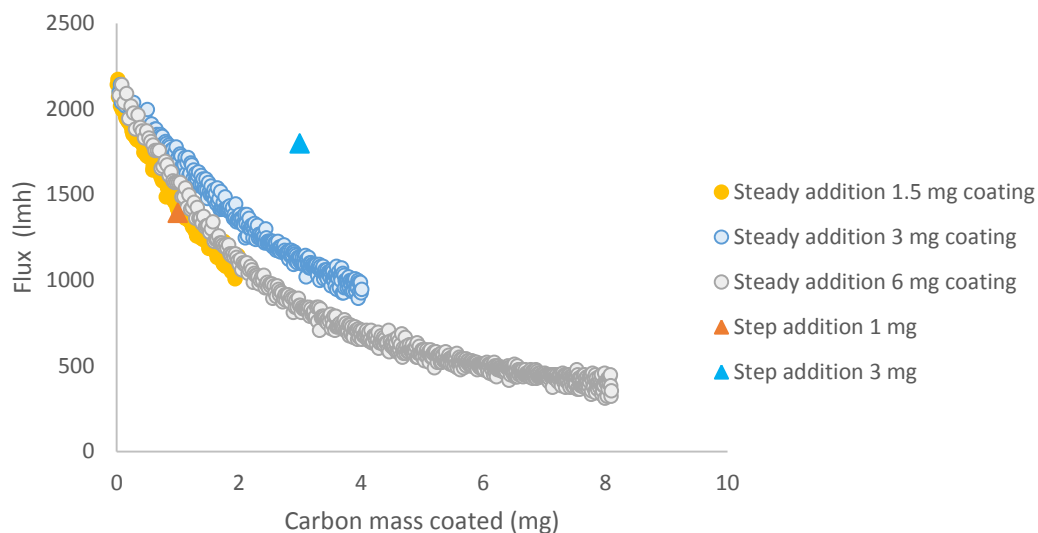


Figure 5.8 Flux data with WC 800 S-PAC added into Amicon cell and pressure vessel. The average DDI water flux was 2099 lmh at 1.5 mg steady addition, 2055 lmh at 3 mg steady addition, 2082 lmh at 6 mg steady addition, 2134 lmh at step addition with 1 mg coating, 2278 lmh at step addition with 3 mg coating.

Table 5.1 shows the membrane resistance due to carbon coating. Since the activated carbon could foul the membrane to some extent, the membrane resistance was calculated and compared. From the data, the resistance of S-PAC is ten times that of the PAC resistance.

Table 5.1 Membrane resistance data with different carbon addition methods

	Membrane resistance (m^{-1})	Membrane resistance due to coating (m^{-1})
PAC added into pressure vessel	1.3×10^{12}	1.9×10^{11}
PAC added into Amicon cell	1.8×10^{12}	2.6×10^{11}
S-PAC added into pressure vessel	1.4×10^{12}	1.3×10^{12}
S-PAC added into Amicon cell	1.2×10^{12}	2.3×10^{12}

5.1.8 Comparison of the effect of carbon mass

Comparison of different carbon mass can help determine the amount of mass needed to use in the NOM experiments since there exists a balance between better

removal for larger amount of carbon and less fouling for smaller amount of carbon. The carbon was added into the pressure vessel in this experiment (Figure 5.9). The carbon mass shown in the legend is the real coated mass. The total mass added into the pressure vessel was double the amount coating the membrane. As shown, the flux decline is more severe with increasing amounts of carbon. Since more carbon particles existed in the system, the probability of carbon in the membrane pores was enhanced. From the data, after 400 mL of permeate solution, the fouling caused only 30% flux decline with a coating of 1.5 mg carbon. Given the results, 1 mg of coating carbon was chosen in the NOM experiment.

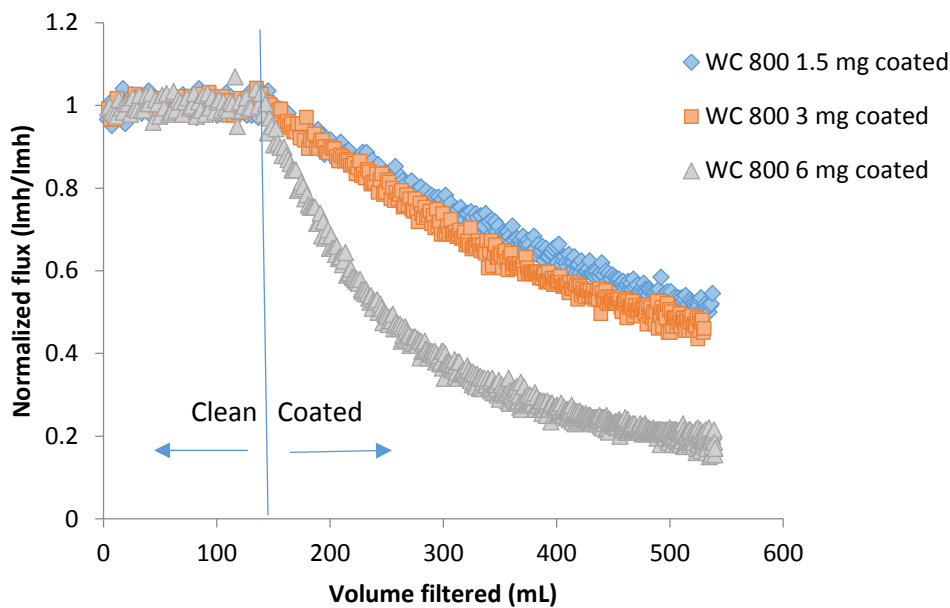


Figure 5.9 Flux data with various S-PAC mass at the pressure of 10 psi. The carbon stock was probe sonicated at 50% power and 5minutes before using, and added into pressure vessel. The average DDI water flux was 2099 lmh for experiment with 3mg WC 800, 2055 lmh for experiment with 6mg WC 800, 2082 lmh for experiment with 12mg WC 800.

5.2 Competitive Adsorption between SOCs and NOM

This section reports the removal of SOCs by PAC and S-PAC. The first sub-section is a comparison of coating versus continuously stirred tank reactor (CSTR) mixing.

Further experiments were done with coating only, as it proved to be advantageous over the CSTR approach. Experiments were conducted in both DDI water and with background NOM to explore the effects of NOM competition. The main hypothesis is that S-PAC is beneficial not only because it results in faster adsorption kinetics, but because NOM does not compete as well with SOCs when S-PAC is used.

5.2.1 Comparison of the adsorption capacity between coating technique and stirred cell technique

Figure 5.10 shows the permeate atrazine concentration with coating and stirred cell method separately. The adsorption capacity of atrazine was better with S-PAC than with PAC in both the stirred cell and coating methods. For the stirred cell method, the removal was the same as the coating method for the first permeate time point but was worse after that. Even though the theoretical contact time in the stirred cell was higher than in the coating case, the coating provides more direct contact between contaminants and carbon, with virtually no need for convection/diffusion in the bulk water to transport contaminants to the carbon surface. These experiments verified what was found previously by Ellerie et al. (67). Thus, the coating technique was chosen as the adsorbent addition method for the remaining experiments.

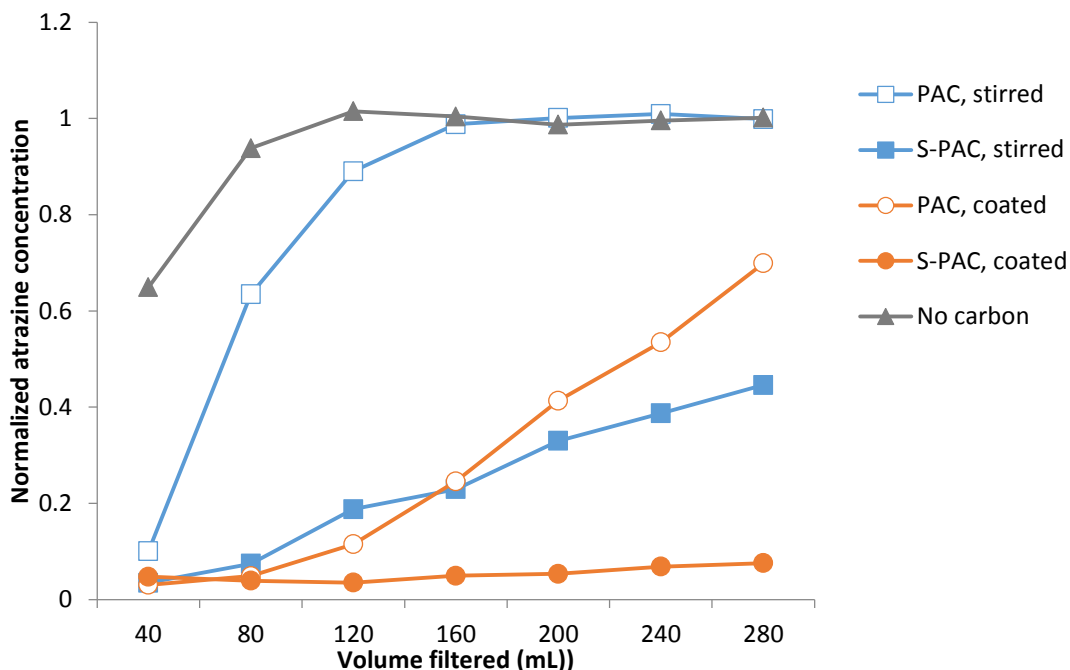


Figure 5.10 Comparison of atrazine removal using the membrane coating technique and the stirred cell technique for 1 mg of WC 800 in both PAC and S-PAC forms. The feed solution was radiolabeled atrazine at 15 ppb in Edisto River water with 4 ppm DOC.

5.2.2 Comparison of the adsorption with and without NOM

For better understanding of NOM competition and run-to-run variability, an NOM experiment was duplicated (Figure 5.11). When the NOM was present in the water matrix, the permeate concentration was lower than that without NOM, which suggested that NOM did compete for adsorption sites with atrazine on the carbon surface. It demonstrated that S-PAC had better adsorption efficiency than PAC both in Edisto River water and in DDI water, which is consistent with Bakkaloglu's result (78). The dominance in Edisto water was more apparent than in DDI water. Comparing Figure 5.12 and 5.13, different concentrations of atrazine in DDI are shown. Blue spots in Figure 5.10 is the 15 ppb atrazine data and Figure 5.13 shows the 150 ppb atrazine data. When the concentration of atrazine was 15 ppb, the atrazine was almost fully adsorbed by carbon.

However, the removal of atrazine was dramatically decreased when the concentration of atrazine increased.

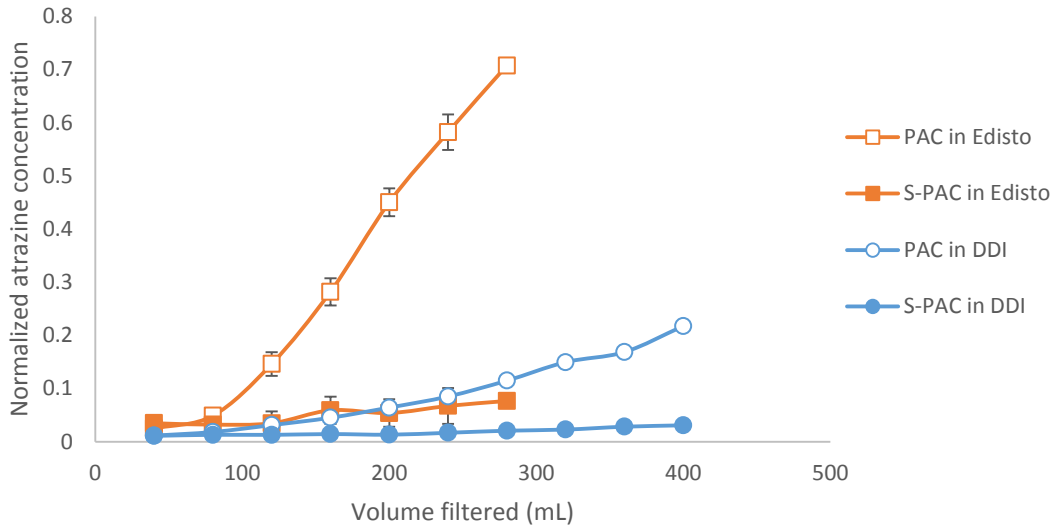


Figure 5.11 Comparison of 1 mg of WC 800 in both PAC and S-PAC forms using the membrane coating technique. The feed solution was radiolabeled atrazine at 15 ppb in both Edisto water with 4 ppm DOC and DDI water. Duplicate results of the Edisto experiment are shown by the error bars (actual values for each replicate lie at the end of the error bars).

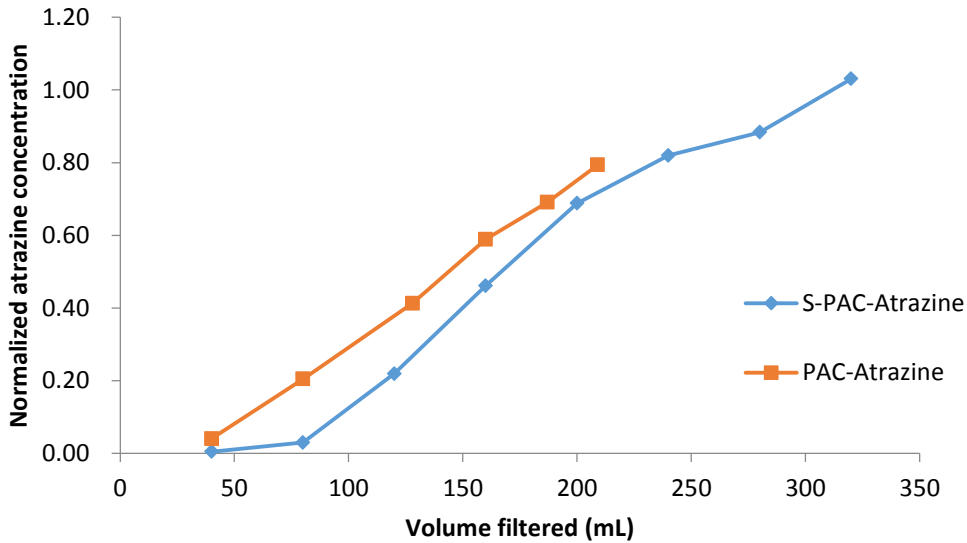


Figure 5.12 Comparison of the adsorption between WC 800 PAC and S-PAC forms using the membrane coating technique. The feed solution was radiolabeled atrazine at 150 ppb in Edisto water with 4 ppm DOC.

5.2.3 Comparison of adsorption with different carbon

Figure 5.14 shows that in DDI water Norit 20B did not remove atrazine as efficiently as WC 800, which was true for both PAC and S-PAC. It is clear, however, that both Norit 20B and WC 800 had better removal efficiency in their S-PAC forms than as PAC. Previous research (71) has concluded that smaller adsorbent particles had faster adsorption kinetics because of shorter travel distance for intraparticle radial diffusion and larger specific surface area per mass. This can not only explain the reason of better removal efficiency on S-PAC, but also the better adsorption of WC 800 than Norit 20B because of the difference in particle size. The S-PAC from WC 800 had a smaller average particle size (0.2 μm) than Norit 20B (0.43 μm). The dominance of the WC 800 S-PAC is apparent. The reasons are unclear, but may have to do with the fact that the Norit 20B S-PAC was milled for a much longer time than the WC 800. The pore structure in Norit 20B may have been destroyed, reducing its adsorption capacity. The effects of milling conditions on S-PAC creation are the subject of continuing work by the research group.

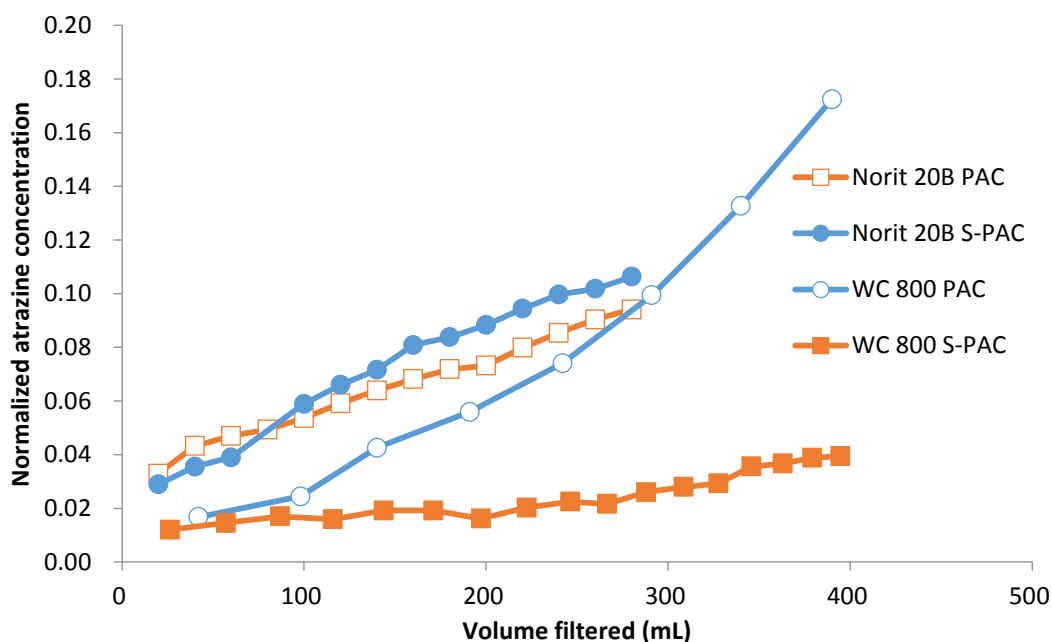


Figure 5.13 Comparison of WC 800 and Norit 20B in both PAC and S-PAC forms at 1 mg in the membrane coating technique. The feed solution was radiolabeled atrazine at 15 ppb in DDI water.

Figure 5.15 compares the adsorption of Norit 20B and WC 800 in the presence of NOM. In Edisto River water Norit 20B did not remove the atrazine as efficiently as WC 800 did whether S-PAC or PAC was used, which is the same tendency with that in DDI water. Also, the natural organic matter competes for the adsorption sites with atrazine since permeate normalized atrazine concentration in Edisto River water was about ten times higher than that in DDI water. For instance, when the filtered volume is 250 mL, the normalized atrazine concentration in WC 800 PAC with Edisto River was about 0.6 while that with DDI was about 0.07. As we know, macro molecules can hinder diffusion by pore blocking. It seems more severe in PAC than in S-PAC. The target molecules are not well adsorbed by activated carbon if the size of the adsorbate is larger than the carbon pores. However, when the adsorbents are PAC, the size difference between NOM and

adsorbent is not as large as that about S-PAC. Because of that, the competition with S-PAC is not as severe as that with PAC.

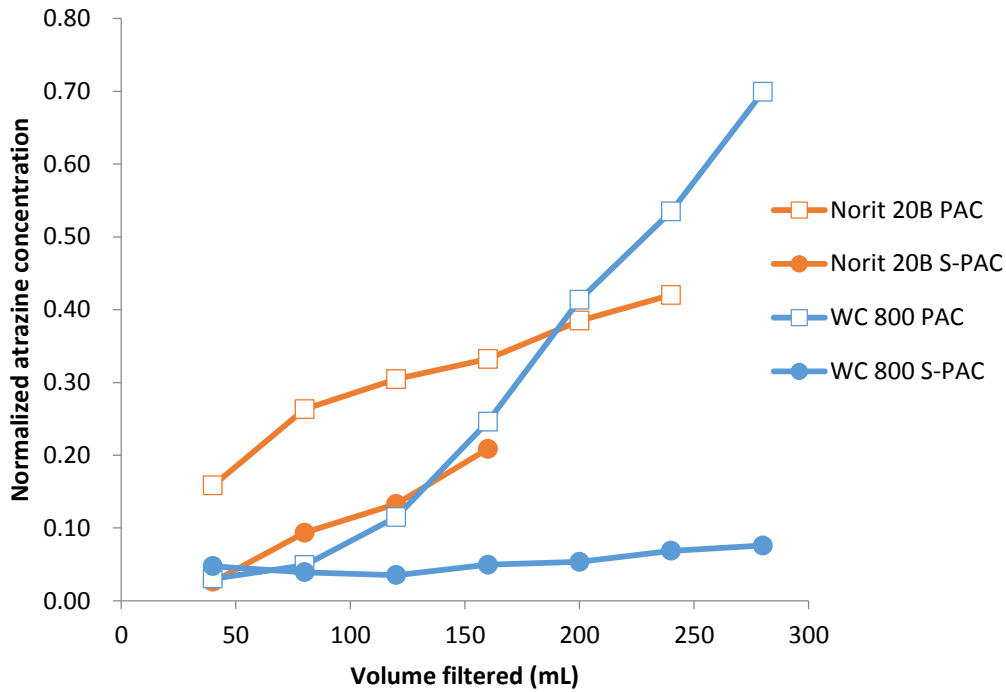


Figure 5.14 Comparison of WC 800 and Norit 20B in both PAC and S-PAC forms at 1 mg in the membrane coating technique. The feed solution was radiolabeled atrazine at 15 ppb in Edisto water with 4 ppm DOC.

Table 5.2 compares the EBCT and carbon usage for Norit 20B and WC 800, PAC and S-PAC. From literature (72), the average EBCT of GAC is 5-10 min. Since in this project, the removal is so excellent with S-PAC that no breakthrough was shown in the experiment. Instead of the more typical breakthrough of 50%, the EBCT of 90% removal was shown which is much more rapid than traditional GAC column. From previous studies, GAC usage rate was around 85 to 100 L/g in carbon adsorbers (73). Essentially,

these experiments are very small scale adsorbers, but because of the fast adsorption kinetics, the CURs for S-PAC are better. S-PAC has large carbon usage and shorter EBCT than PAC for both type of carbon. With the short EBCT, the CUR is still high and the removal is excellent with this thin membrane column. WC 800 has better carbon usage than Norit 20B. WC 800 also has shorter contact time than Norit 20B.

Table 5.2 EBCT, BV, and CUR with Norit 20B and WC 800. The EBCT is calculated by 90% removal of SOCs.

Carbon Type		EBCT (min)	BV	CUR (L/g)
Norit 20B with NOM	PAC	9.0×10^{-3}	10,000	25
	S-PAC	3.0×10^{-3}	30,000	75
WC 800 with NOM	PAC	2.0×10^{-3}	40,000	100
	S-PAC	8.0×10^{-4}	112,000	280
WC 800 without NOM	PAC	9.4×10^{-4}	100,000	250
	S-PAC	5.9×10^{-4}	160,000	400

5.2.4 Flux data with and without NOM

A study (74) observed that the system with S-PAC actually showed less fouling because of its stronger flocculation ability and increased propensity for removal of NOM, a membrane foulant. Another study (75) suggested that NOM with chromophoric properties was adsorbed onto external sites in activated carbon so that the adsorption on smaller particles of S-PAC was greater. Since NOM can be well adsorbed onto S-PAC, the fouling caused by NOM in S-PAC experiment is weaker. From Figure 5.16, the flux in DDI with PAC did not change compared to clean water flux, just the same with the no carbon run in DDI. However, when NOM was present without adsorbents, the flux dropped throughout the run until nearly reaching zero flux. With either PAC or S-PAC the adsorbents helped slow the flux decline that otherwise would have occurred without their protective coating. The fouling driving at the beginning was S-PAC since NOM was

not too much. As NOM accumulated on the membrane, the flux decline for the solutions containing NOM continued and NOM was clearly the main driving force for the decline. On the other hand, the flux for S-PAC in DDI stabilized and remained at about 50% for the remainder of the experiment. However, any advantage for S-PAC in the presence of the Edisto NOM was not evident because its flux decline was similar to that of PAC in the presence of the Edisto NOM.

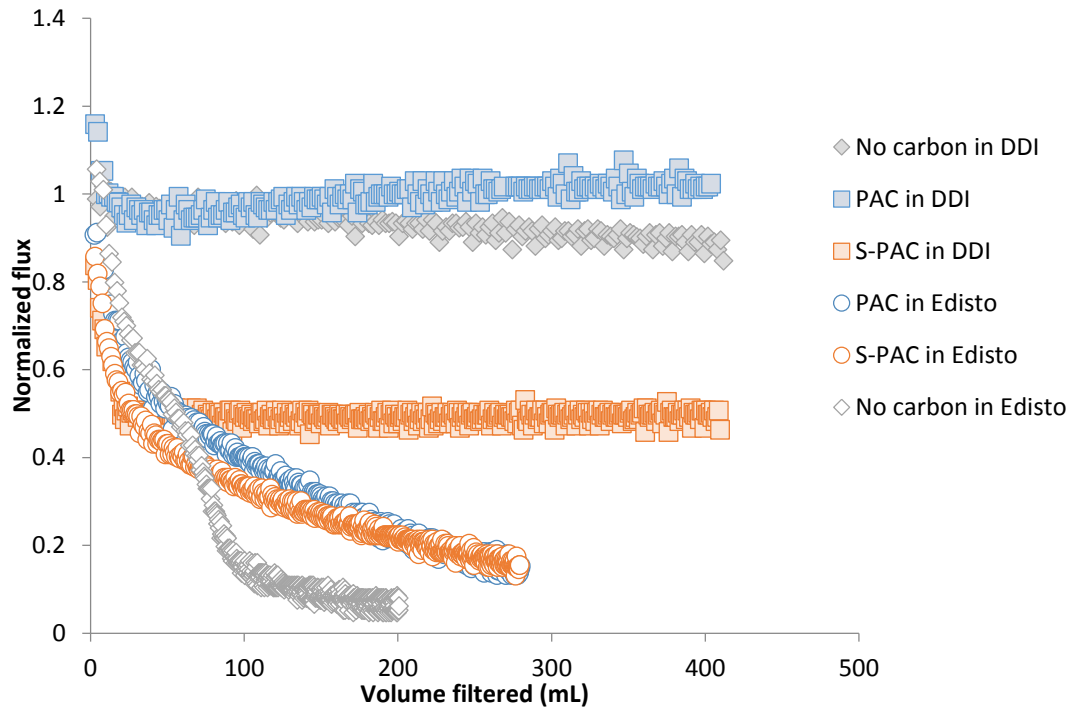


Figure 5.15 Comparison of the normalized flux values for 1 mg of WC 800 in both PAC and S-PAC forms in the membrane coating technique. The feed solution was radiolabeled atrazine at 15 ppb in both Edisto water with 4 ppm DOC and in DDI water.

5.2.5 Flux data for different carbons

From Figure 5.17, the flux decline of Norit 20B and WC 800 was compared. When in Edisto water, the flux in S-PAC decreased faster at the first 100 mL filtered volume.

As time continued, the NOM became the dominant factor that caused fouling. The same conclusion can be drawn from Figure 5.16, which shows the flux decline for two different carbons in the presence of the Edisto NOM. The flux with Norit 20B S-PAC began from 60% of the clean water flux, which needs to further study. In addition, the fluxes with Norit 20B decline faster than those with WC 800, which means the anti-fouling behavior of WC 800 is better than that of Norit 20B. Therefore, the type of carbon used to prepare the S-PAC has effect.

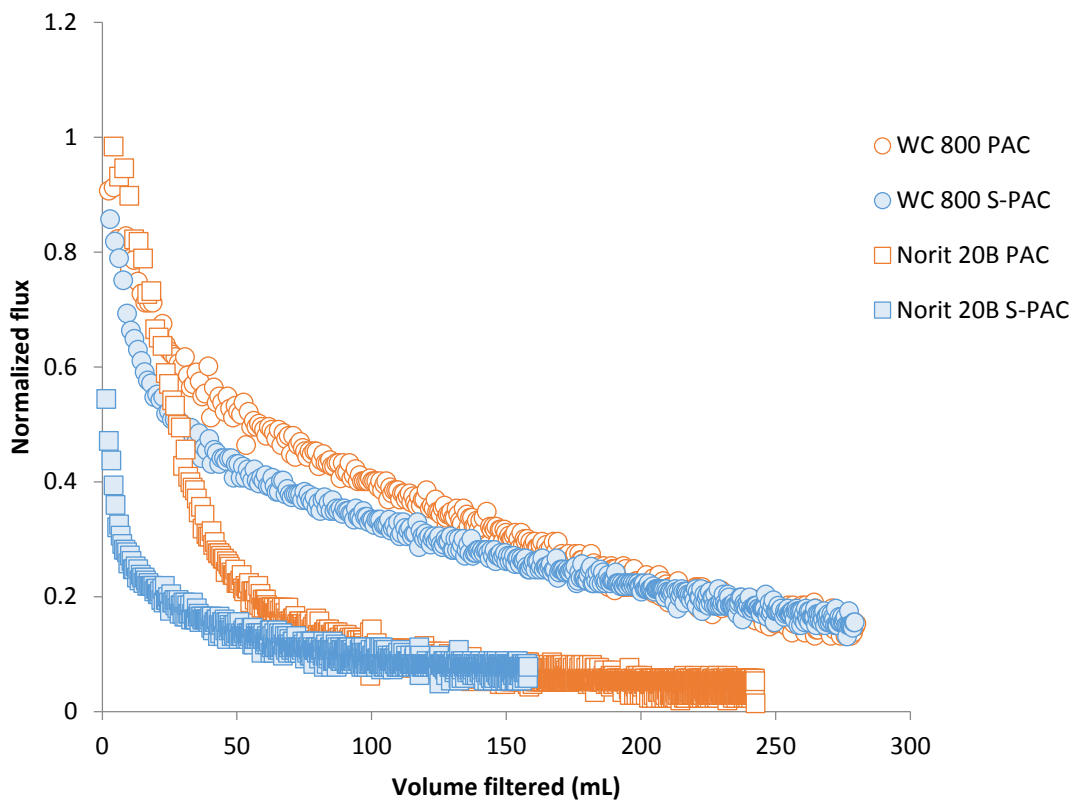


Figure 5.16 Comparison of normalized flux for 1 mg of WC 800 and Norit 20B in both PAC and S-PAC forms in the membrane coating technique. The feed solution was radiolabeled atrazine at 15 ppb in Edisto water with 4 ppm DOC.

5.2.6 Carbamazepine data

Figure 5.18 shows the carbamazepine data with WC 800 PAC and S-PAC. The adsorption capacity of carbamazepine was greater with S-PAC than PAC, which is consistent with the atrazine data. Figure 5.19 presents the comparison between atrazine and carbamazepine.

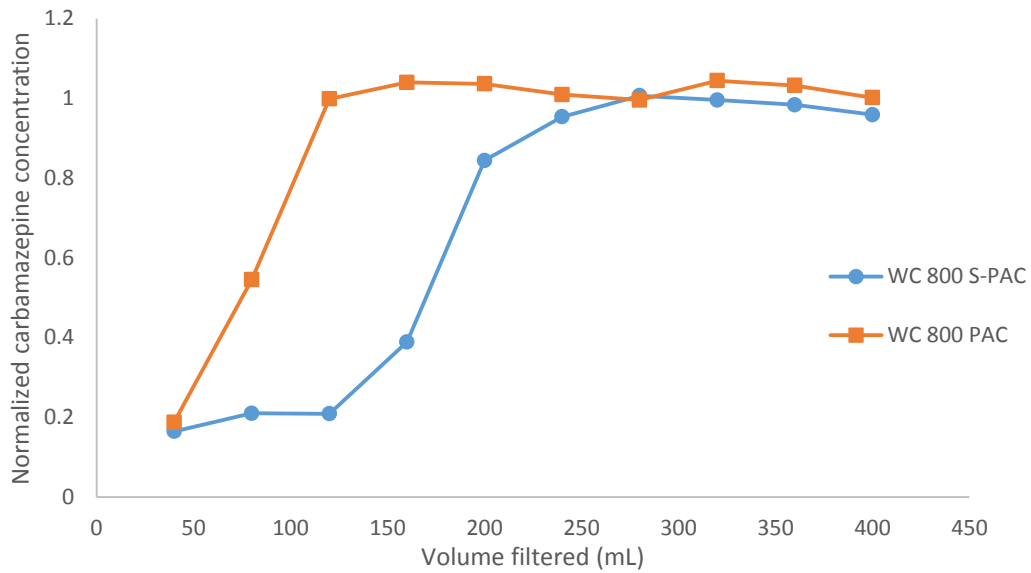


Figure 5.17 Comparison of the WC 800 in both PAC and S-PAC forms with 1 mg in the membrane coating technique. The feed solution was carbamazepine at 1000 ppb in Edisto water with 4 ppm DOC.

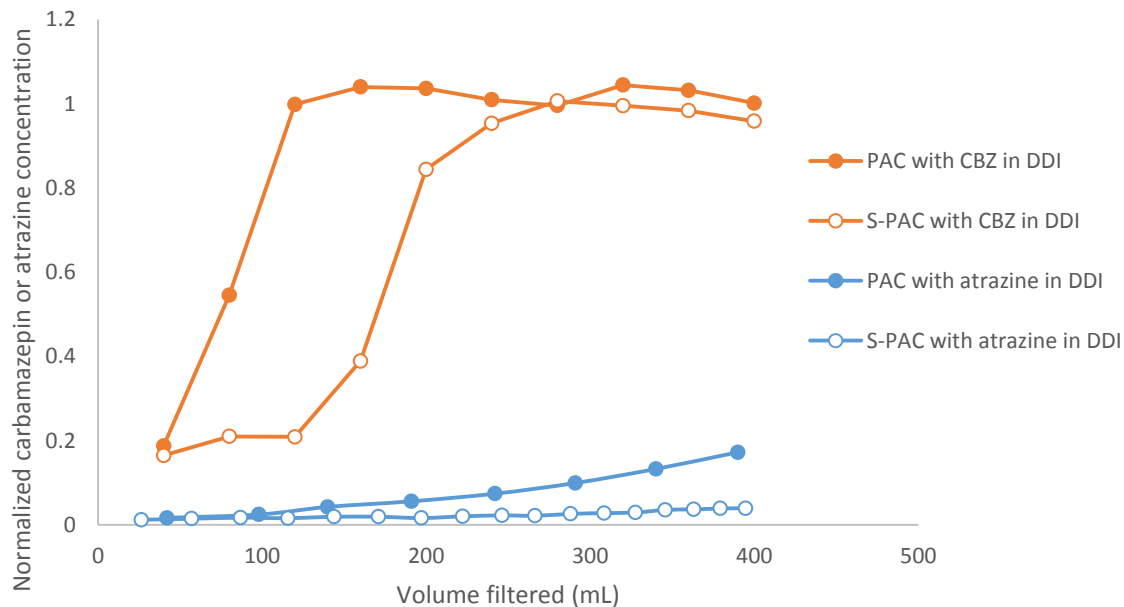


Figure 5.18 Comparison of WC 800 PAC and S-PAC (1 mg coating) for adsorption of atrazine and carbamazepine. The feed solution was atrazine at 15 ppb or carbamazepine at 1000 ppb in Edisto water with 4 ppm DOC.

Figure 5.20 compares the adsorption capacity of carbamazepine with and without NOM. Since the concentration of carbamazepine was higher than atrazine, the difference of removal efficiency was not so clear as with atrazine. However, the breakthrough can also reflect the removal. In the presence of NOM, the removal was less when compared to the results of DDI run. Also, S-PAC still showed better removal than PAC. For carbamazepine, the removal by S-PAC in the presence of NOM was greater than the PAC removal efficiency in DDI water.

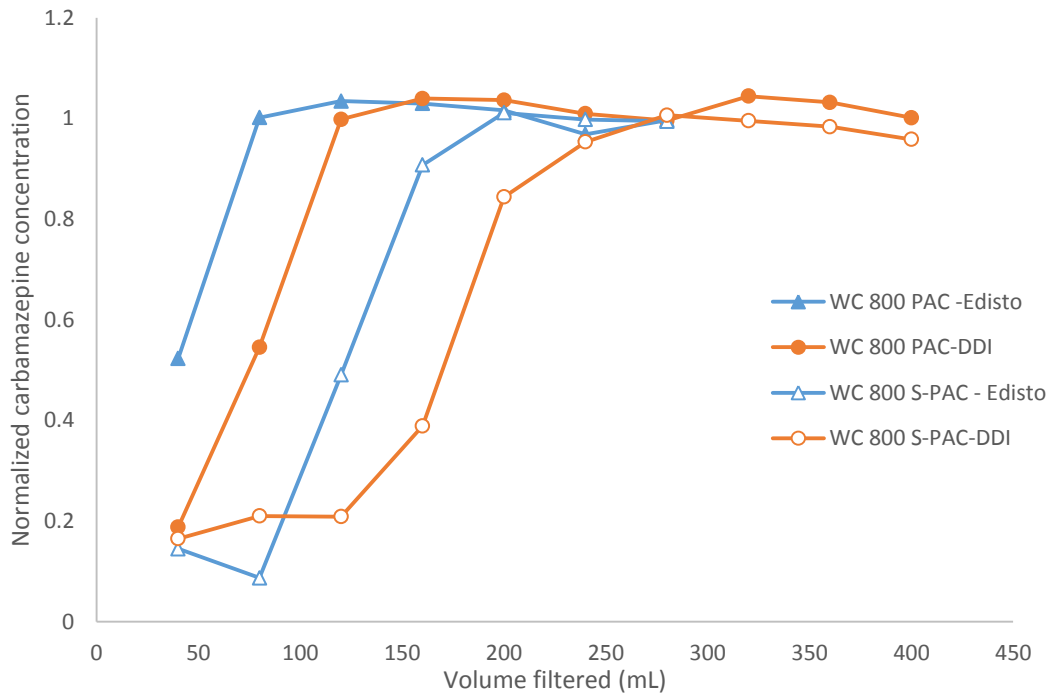


Figure 5.19 Comparison of WC 800 PAC and S-PAC (1 mg) with the membrane coating technique. The feed solution was carbamazepine at 1000 ppb in Edisto water with 4 ppm DOC and DDI water.

5.2.7 Effects of NOM concentration

As suggested previously, based on literature and experimental results of this thesis, NOM competition and are related to many factors including NOM concentration and pH. Figure 5.21 shows the atrazine removal in the presence of different concentrations of SRNOM. In contrast to the results with the Edisto River NOM, SRNOM did not compete with atrazine adsorption greatly since the permeate atrazine concentration was still low in S-PAC run. S-PAC has larger external surface area than PAC. Different NOM concentration effects on carbon adsorption and contaminant competition may be related to various internal and external adsorbent particle surface. According to the conclusion of Matsui et al. (76), PAC and S-PAC can adsorb a similar amount of NOM that will

compete with the contaminant being removed. However, S-PAC can load more NOM that does not compete with contaminant in the external adsorption sites than PAC.

Besides, from the PAC data, the decreasing of adsorption capacity with increasing NOM concentration was observed. Since the adsorption of contaminant decreases more rapidly on PAC as NOM concentrations increases, the external sites and conformation on S-PAC may favor SOC adsorption.

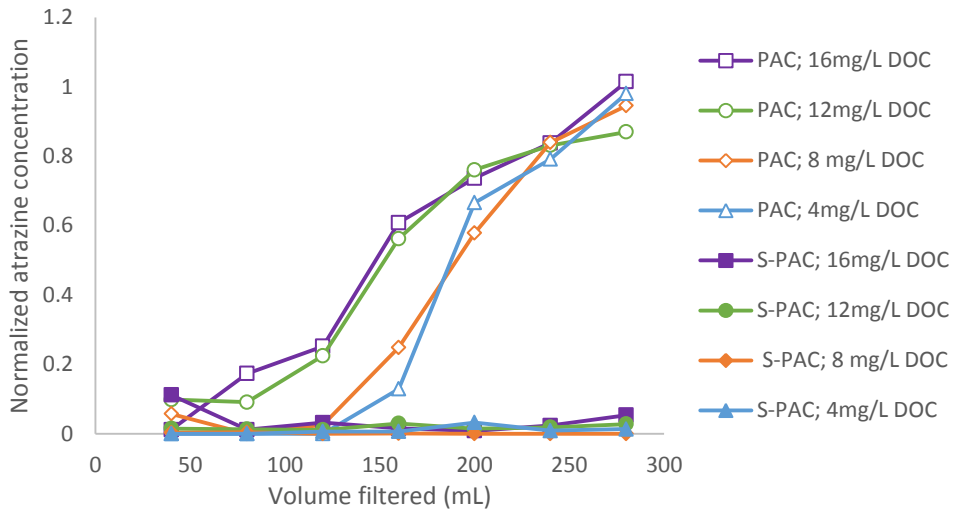


Figure 5.20 Comparison of atrazine removal by a 1 mg coating of WC 800 in both PAC and S-PAC forms with different SRNOM concentrations. The atrazine concentration was 15 ppb.

Permeate NOM concentration is shown in Figure 5.22. The NOM concentration of feed solution did not have much effect on the carbon adsorption. The PAC and S-PAC did not have better NOM adsorption compared to the SOCs. It is clear that SRNOM did not prevent the atrazine adsorption which occurred mostly on the internal sites of the adsorbents. Also, after a few NOM molecules were adsorbed on the external sites, the adsorption of NOM was at capacity and NOM would not be adsorbed any more. Unlike

the other NOM concentrations, the 16 mg/L DOC is more stable, which requires further study.

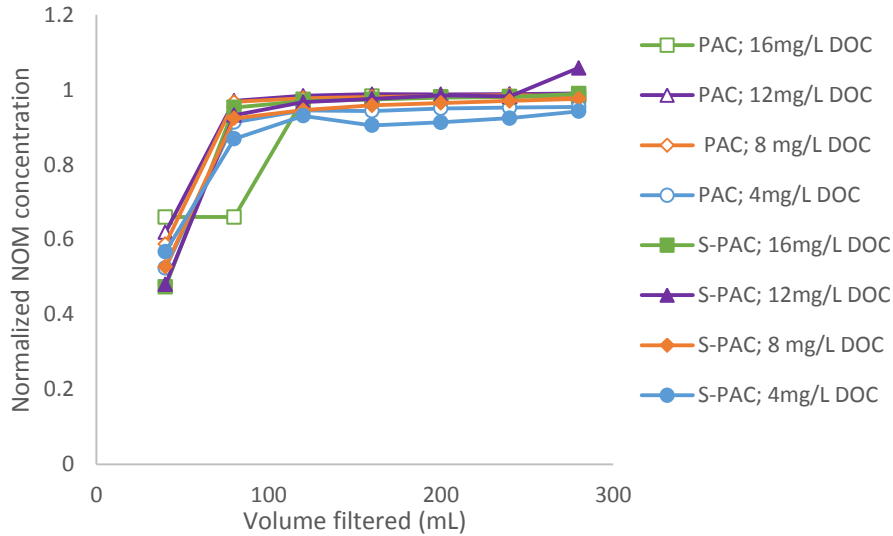


Figure 5.21 Comparison of NOM removal by 1 mg coatings of WC 800 PAC and S-PAC. The experiment was repeated for different SRNOM concentrations. The feed atrazine concentration was 15 ppb. These are the NOM data from the same experiments for which atrazine data were plotted in Figure 5.20.

From the flux data in Figure 5.23, SRNOM caused less than thirty percent of the fouling, unlike the rapid drop in flux of Edisto water NOM (Figure 5.16). WC 800 S-PAC caused around fifty percent of fouling without any NOM (Figure 5.16). Thus, in the S-PAC and SRNOM system, the flux decline was more than thirty percent although some part of NOM was adsorbed by S-PAC. In this case, the S-PAC is the main reason for the fouling. As the NOM concentration increased, the fouling was more severe but not much obviously. The reason is that SRNOM cannot lead to severe fouling because of the molecular size.

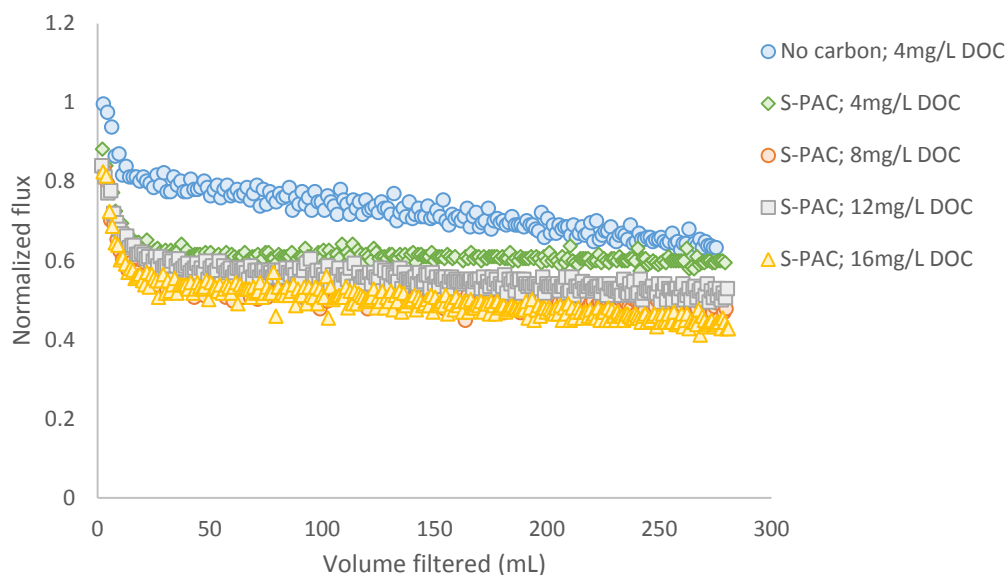


Figure 5.22 Flux comparison for 1 mg coatings of WC 800 S-PAC with different SRNOM concentrations. The atrazine concentration was 15 ppb.

Figure 5.24 shows the flux in the PAC plus SRNOM system. Like S-PAC data, the fouling with PAC was more severe than that without adsorbents. It is noteworthy since PAC itself will not cause fouling. As Figure 5.22 presents, PAC can adsorb NOM to some extent. Further experiments need to be run to confirm the mechanisms of this phenomena. A similar tendency was observed with S-PAC and SRNOM in which increasing fouling with increased NOM concentration did not show obviously due to the certain size range of SRNOM.

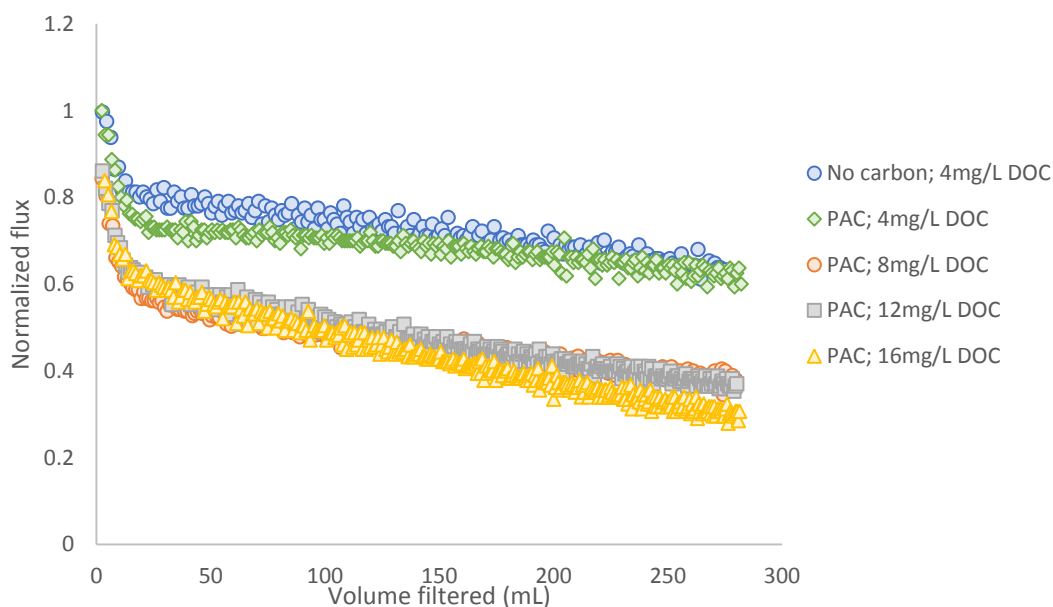


Figure 5.23 Comparison of flux decline for 1 mg of WC 800 PAC with different SRNOM concentrations using the membrane coating technique. The atrazine concentration was 15 ppb.

5.2.8 Effects of pH

An increase in pH causes the ionization of the carboxyl groups that improves the intramolecular repulsion and solubility. At low pH conditions, carboxyl groups of NOM are protonated and form large complexes which is neutral charge. Also, large complexes will easily be adsorbed by carbon and block the pores. Given the pH behavior of NOM, the competition between NOM and SOCs is more severe at low pH than at high pH conditions. Figure 5.25 and Figure 5.26 show the S-PAC and PAC adsorption of atrazine, respectively. Both graphs are consistent with the competition mechanism described above. For S-PAC, the atrazine was adsorbed well at the beginning in all the runs. At the first 200 mL, the difference in adsorption is larger. In pH 3 circumstance, adsorption capacity of atrazine is the weakest. The pH 11 run maintained excellent removal up to 280 mL. In all, due to the formation of large complexes at lower pH, the NOM was easily

to be adsorbed by the carbon. Then, the adsorption capacity of atrazine decreased as the competition grew more severe.

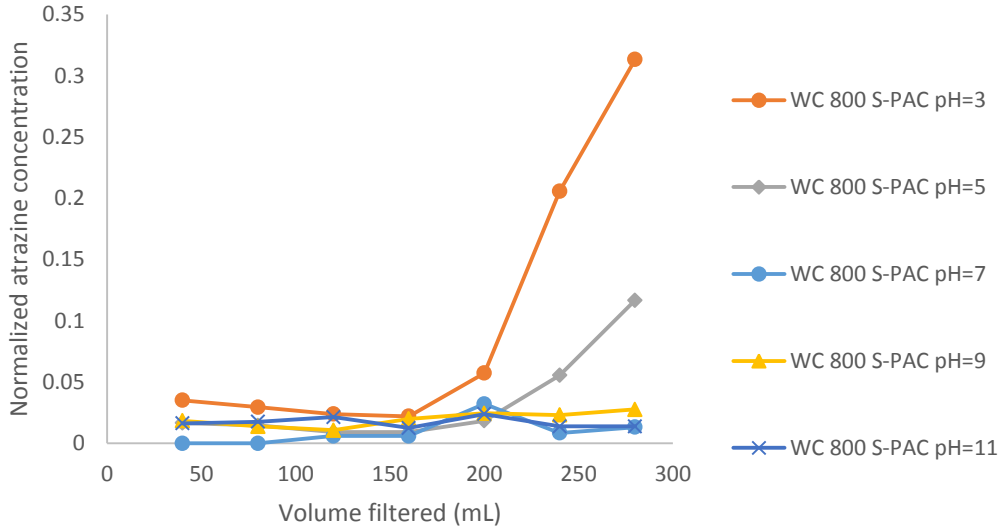


Figure 5.24 Atrazine removal comparison at different pH values for 1 mg of WC 800 S-PAC coatings in the presence of NOM. The atrazine and SRNOM concentrations were 15 ppb and 4 ppm DOC, respectively.

In Figure 5.25, the removal of atrazine did not shown much difference both at the beginning and at the end. However, the middle part of the adsorption showed the difference. Similar to the S-PAC removal, pH 3 and pH 5 had the least adsorption capacity, and followed by pH 7. Similar to that of pH 7. At pH 9, the removal was the best. Since the breakthrough was faster for PAC compared to S-PAC, permeate concentrations were equal to feed concentration at the end. The initial removal was greater than later in the run, which was similar to the results with Edisto NOM (Figure 5.12).

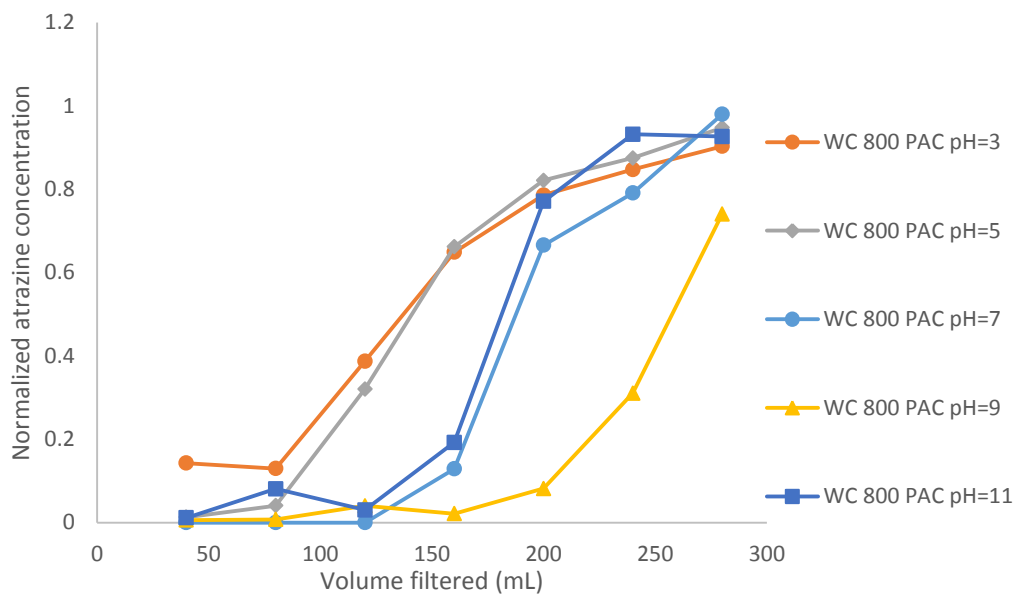


Figure 5.25 Atrazine removal for 1 mg coatings of WC 800 PAC with different pH in the presence of NOM. The feed atrazine concentration was 15 ppb in SRNOM with 4 ppm DOC.

Figure 5.27 and Figure 5.28 show the removal of NOM in S-PAC and PAC, respectively. For S-PAC removal, in contrast with the atrazine data, the removal capacity for NOM was greater as the pH decreased. With PAC, the results were same. The competition of NOM and SOCs was more severe when pH was low. As a result, the removal of NOM was more and removal of atrazine was less when pH was low.

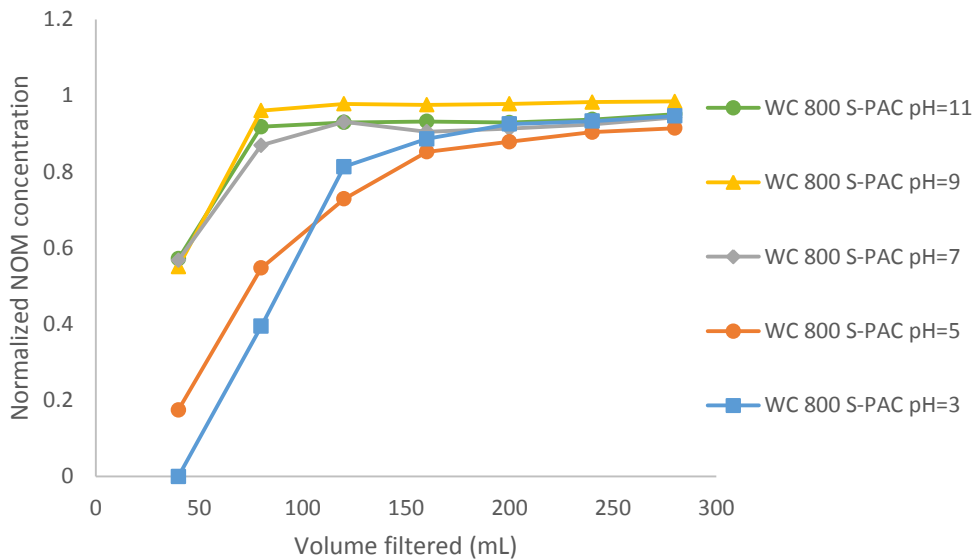


Figure 5.26 NOM removal for a 1 mg coating of WC 800 S-PAC at varying pH. The atrazine concentration was 15 ppb in SRNOM with 4 ppm DOC.

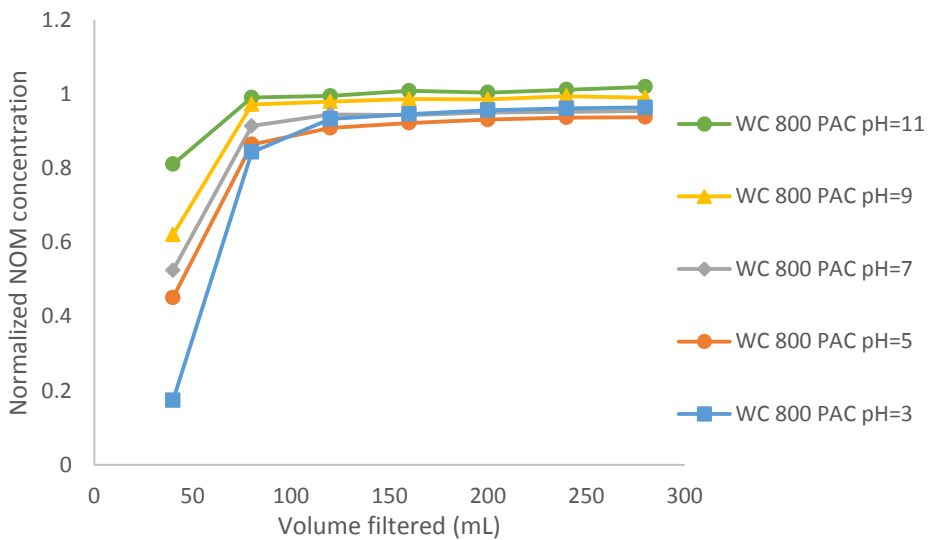


Figure 5.27 NOM removal for 1 mg coatings of WC 800 PAC at varying pH. The atrazine concentration was 15 ppb in SRNOM with 4 ppm DOC.

Figure 5.29 and Figure 5.30 show the flux data at various pH with PAC and S-PAC, respectively. In both PAC and S-PAC runs, the flux decline was the greatest when

pH was high. Since the NOM removal reached breakthrough quickly and after that there was no NOM adsorbed, the results of the pH variation require further understanding. It is interesting to note that when pH was high, the flux decline was severe. It can be assumed that at lower pH the carbon coating was removed foulants more readily and thus protected the membrane pores. Further research should be conducted to confirm the mechanisms of NOM and membrane interactions with different pH. The SOC_s and NOM should be run in the membrane/no carbon system to learn the impact of pH. Another experiment should be conducted with natural water NOM.

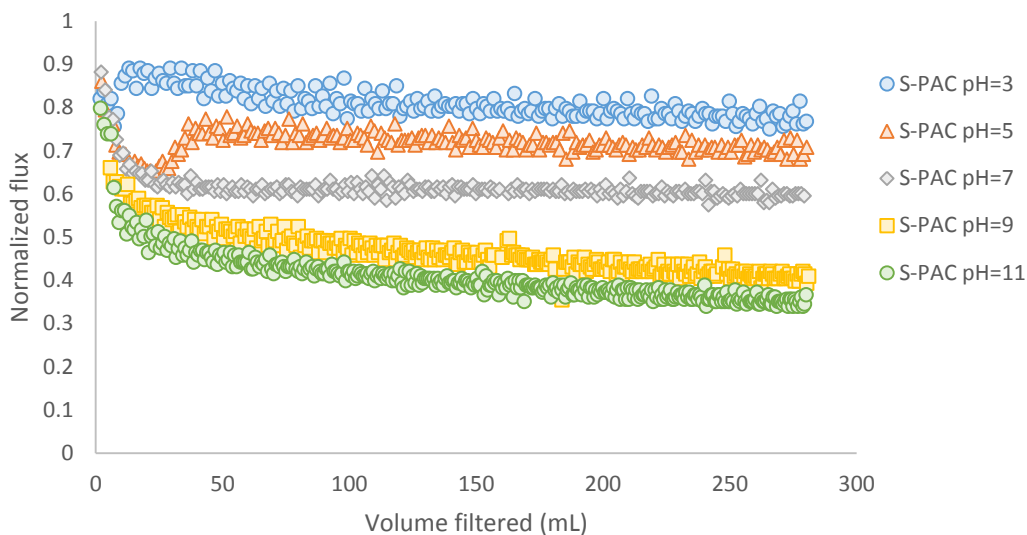


Figure 5.28 Flux comparison for 1 mg coatings of WC 800 S-PAC at varying pH. The atrazine concentration was 15 ppb in SRNOM with 4 ppm DOC.

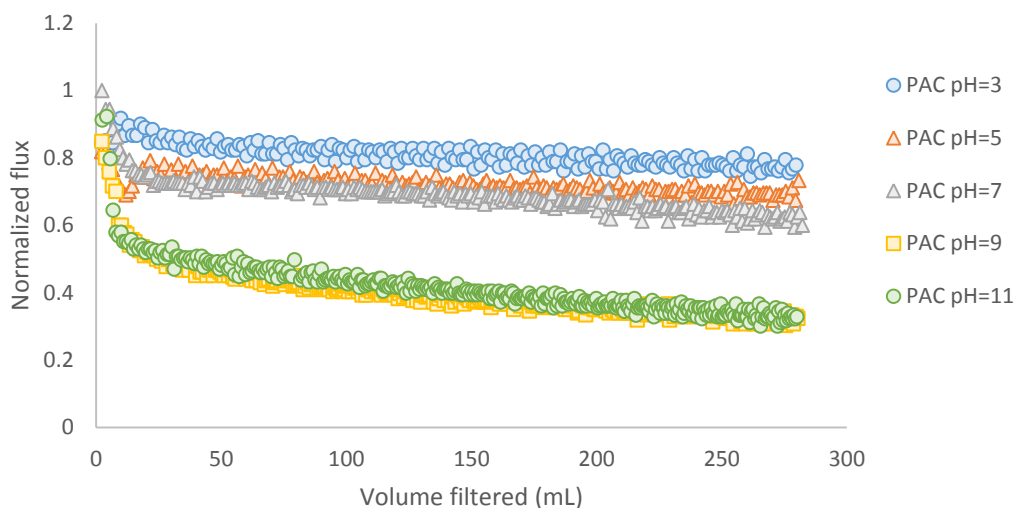


Figure 5.29 Flux comparison for 1 mg coatings of WC 800 PAC with varying pH. The atrazine concentration was 15 ppb in SRNOM with 4 ppm DOC.

5.2.9. Caveats concerning contact times

During the NOM competition experiments, the carbon amount added into the Amicon cell was maintained at 1 mg. Bath sonication was operated to PAC in one hour and probe sonication was operated to S-PAC at fifty percent power in five minutes. The pressure kept at 10 psi.

Although data collected under constant flux are more reliable, constant pressure was used because the flux data were an important aspect that we want to know. Since the flux decline leads to longer contact time, more SOC removal will occur, which was a limitation in the experiment design. If that happens, the SOC breakthrough will get longer and the discussion based on the various removal will be not reliable. But, in many cases, when the flux is low, the SOC breakthrough is fast. So the constant pressure is still

reliable and worth to discussing. According to that, if the constant flux experiments do, more dramatic differences between samples will show and S-PAC would be favored even more.

Chapter 6 CONCLUSIONS AND RECOMMENDATIONS

6.1 Conclusions

The main conclusions are provided in five subsections below, which are tied to the five objectives in Chapter 3.

(1) *Compare membrane flux decline with PAC and S-PAC, including aggregation effects.* Flux decline by carbon coatings was directly related to the particle size. The PAC used had a large enough particle size so as to not dramatically reduce flux. S-PAC did reduce flux because its particle size was similar to the membrane pore size, but the aggregation state was also important in determining the level of flux reduction. Aggregation occurred when the highly concentrated (slurry) S-PAC was stored as a wet solution. Using a bath sonicator or probe sonicator can help carbon particles disaggregate and disperse in the solution. Compared to the bath sonicator, the probe sonicator disaggregated the particles in a shorter time. The bulk of the work here was done after samples were sonicated to ensure consistent data regarding the small-particle adsorbents. Depending on the type of carbon, the flux decline caused by S-PAC was from 40% to 60%.

(2) *Evaluate contaminant (SOCs) removal for PAC and S-PAC in deionized water.* Both atrazine and carbamazepine showed better removal with S-PAC than PAC, likely due to the faster adsorption kinetics in the small particles of S-PAC. S-PAC has more external surface area, meaning contaminants need not travel deep into the particle to find adsorption sites.

(3) Measure contaminant (SOCs) removal when NOM is present. NOM had a marked effect on contaminant removal, decreasing the adsorption rate and thus shortening the time to breakthrough. The effects were more obvious for PAC than S-PAC, indicating that NOM competition is reduced with S-PAC. NOM can be adsorbed to a greater degree on S-PAC than PAC since the NOM was more easily attached on the external sites of adsorbents and the external surface area of S-PAC was larger. But even with that, competition was lower with S-PAC.

(4) Evaluate flux decline in the presence of NOM. Comparing the PAC and S-PAC experiments, the flux dropped faster in the S-PAC runs initially since the S-PAC caused a certain amount of fouling. After initial part of the filtration run, the Edisto NOM experiments showed that the accumulated and became the main driving force of the flux decline. Then, instead of being detrimental to the flux, the S-PAC was beneficial, helping to prevent the flux decline observed in the absence of S-PAC. This is an important finding; from DDI experiments the hindering of S-PAC on membrane performance is a large concern, but the S-PAC was beneficial to flux performance in natural water experiments. The results were different in the SRNOM case. SRNOM caused less flux decline than S-PAC alone, so S-PAC did not help mitigate the fouling. Also, interestingly, PAC was detrimental to flux in the presence of SRNOM, while it had virtually no flux effect in DDI water. It appears that the character of the NOM was important for the carbon coating-NOM-membrane interactions.

(5) Determine the effects of solution pH and NOM concentration. A hypothesis from the literature (76) was that PAC and S-PAC could adsorb similar amounts of NOM, which competes with contaminant. On the other hand, S-PAC can load more NOM which does not compete with contaminant than PAC in the external adsorption sites (75). In this project, from the PAC data, a decrease in adsorption capacity with increased NOM concentration was observed. Since the adsorption of contaminant decreased more rapidly on PAC when NOM concentration increased, it suggested that the external sites and conformation on S-PAC may be more favorable to small-molecule adsorption (contaminant). For pH effects, low pH likely caused protonation of carboxyl groups, minimizing charge repulsion within NOM molecules so that they could fold into more compact structures. The charge neutralization would also make them more readily adsorbed, as they would have less electrostatic repulsion with carbon surfaces. Both of these mechanistic hypotheses are consistent with the observed data; at lower pH atrazine was removed to a lesser extent, likely due to the ability of SRNOM to reach adsorption sites and to compete strongly with SOCs for the sites. Interestingly, lower pH resulted in less flux decline, which is counterintuitive because one would expect the NOM to adsorb more readily to the membrane and decrease flux to a greater extent at lower pH. The observed results suggested that perhaps at lower pH the carbon coating was able to remove foulants more readily and thus protect the membrane pores.

6.2 Future Work

6.2.1 The effects of ionic strength

The effects of ionic strength should be studied. High ionic strength and the presence of divalent cations can cause more severe membrane fouling as described in the literature review. Adsorption of humic substances on activated carbon also increases with increasing ionic strength (74). Filtration of water with high ionic strength (> 0.1 M) can build salt “screens” and reduce both attractive and repulsive electrostatic interactions. NOM is negatively charged and depends on the electrostatic interactions. If the interactions between NOM and carbon surface is attractive and the concentration on the carbon surface is low, the adsorption will decrease as the ionic strength increases. Conversely, if the interactions are repulsive, increased ionic strength will cause increased adsorption. Besides, the electrostatic interactions between negatively charged membrane and NOM also enhance since the ionic strength increases (77).

If the results indicate that the carbon adsorption will increase as the ionic strength increases, the repulsive interactions between carbon and NOM may be less than occur when membrane and carbon are negatively charged. If the result is the converse, the carbon may be positively charged or the repulsive interactions between carbon and NOM are greater than that with the membrane. The difference in the adsorption mechanisms between PAC and S-PAC can be determined through this research.

6.2.2 Aggregation research

Finding the balance between most adsorption capacity and least fouling is important to treat water and understand the mechanisms of fouling. Since different functional groups are present in different types of carbon and different structures of

carbon can be used, combination of various carbons according to their structure and chemical characteristics can integrate the advantages of greater adsorption capacity and larger size without fouling.

6.2.3 Further experiments of pH effects

In Figure 5.29 and Figure 5.30, the mechanisms of pH influences require further research. The experiments without NOM in different pH water may be conducted to compare the influence of NOM.

6.2.4 Modeling research

Homogeneous Surface Diffusion Model (HSDM) and Linear Driving Force (LDF) Model can be included in future research and adjusted to fit the S-PAC/microfiltration system. From the models, the mechanisms and parameters of adsorption competition can be concluded and confirmed.

APPENDICES

APPENDIX A: Preparation of Radiolabeled Atrazine Stock Solution

1. Calculation of atrazine volume

The concentration of atrazine is 15 ppb (labeled: non-labeled=1:29)

The concentration is not various in this procedure.

Assume the feed solution needed to prepare is 1000 mL

The mass of atrazine is $15 \text{ ppb} \times 1000\text{mL} = 0.015 \text{ mg/L} \times$

$1000\text{mL} \times 1\text{L}/1000\text{mL} = 0.015 \text{ mg}$

Labeled atrazine: $0.015 \text{ mg} \times 1/30 = 5 \times 10^{-4} \text{ mg}$

The stock solution of labeled atrazine is 0.5 mg/L

Non-labeled atrazine: $0.015 \text{ mg} \times 29/30 = 0.0145 \text{ mg}$

The stock solution of non-labeled atrazine is 0.1 mg/mL

The volume of labeled stock solution needed is $5 \times 10^{-4} \text{ mg} / 0.5 \text{ mg/L} = 1 \times 10^{-3} \text{ L} = 1\text{mL}$

The volume of non-labeled stock solution needed is $0.0145 \text{ mg} / 0.1 \text{ mg/mL} = 0.145$

mL

Add the stock solution in volumetric flask and then add DDI to scale mark

2. The preparation of calibration curve

Prepare atrazine at 0 ppb, 0.9375 ppb, 1.875 ppb, 3.75 ppb, 7.5 ppb, and 15 ppb

Take 5 mL stock solution of the volumetric flask and move it to a **plastic** vial

(20mL). Mark this vial as 15 ppb.

Repeat the step above and mark it as 7.5 ppb.

Add 5 mL of DDI into 7.5 ppb vial to make the concentration as 7.5 ppb.

Take the solution of 7.5 ppb vial into a new plastic vial and mark as 3.75 ppb.

Dilute the solution in the vial and repeat the steps above to get the calibration curve.

0 ppb concentration is added 5 mL of DDI.

Add scintillation cocktail into these vials 5 mL per vial.

APPENDIX B: The MDL of Radiolabeled Atrazine with C¹⁴

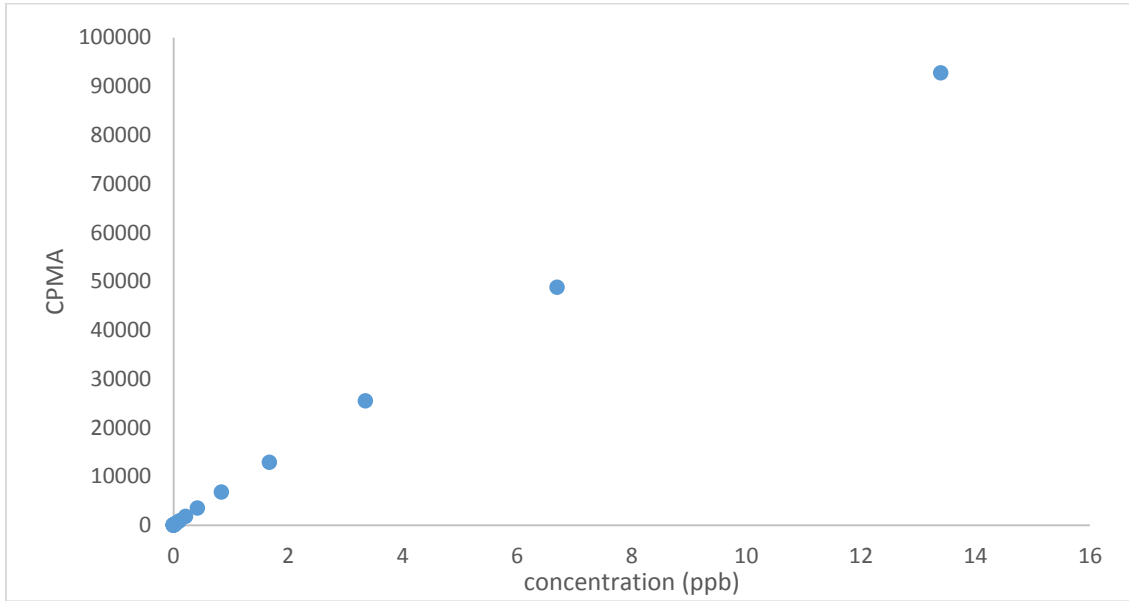


Figure A1 Detection of MDL about new atrazine (the full scale, from 13.4 ppb)

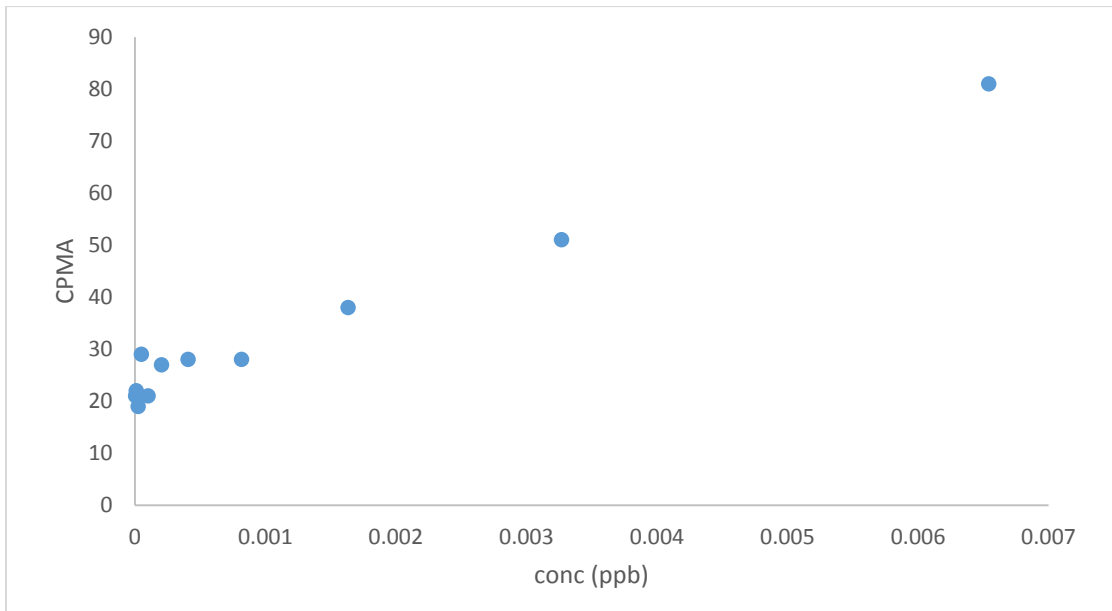


Figure A2 Detection of MDL about new atrazine (the low concentration range, from 0.0065 ppb)

APPENDIX C: Standard Operating Procedure of Amicon Cell

Clean-water flux

1. Cut membranes and soak them in DI water.
2. Place backing and membrane in Amicon cell.
3. Fill pressure vessel with DI water.
4. Use tubing to connect Amicon cell, pressure vessel, and balance. Turn on computer.
5. Open the valve on the nitrogen tank (not connected to pressure vessel) to adjust to target pressure. Close the valve.
6. Connect nitrogen tank to pressure vessel.
7. Press start on Lab View and name the output text file.
8. Crack the valve on the nitrogen tank, allowing the Amicon cell to fill with water. Once full, close the valve on the top of Amicon cell.
9. Open the nitrogen valve all the way.
10. Run until water drains completely or flux decline is <5% change over 20 minutes.
11. Press stop on Lab View and close nitrogen valve.

Sample run

1. Disconnect tubing from Amicon setup (cell and pressure vessel).
2. Remove any leftover DI water from the setup.

3. Fill pressure vessel with sample of interest.
4. Use tubing to connect Amicon cell, pressure vessel, and balance.
5. Connect nitrogen tank to pressure vessel. Do not adjust pressure between clean-water run and sample run.
6. Press start on Lab View and name the output text file.
7. Crack the valve on the nitrogen tank, allowing the Amicon cell to fill with sample. Once full, close the valve on the top of Amicon cell.
8. Open the nitrogen valve all the way.
9. Run until sample drains completely or flux decline is $<1\%$ change of the clean-water flux.
10. Press stop on Lab View and close nitrogen valve.

APPENDIX D: Front Panel of LabView Software Interface

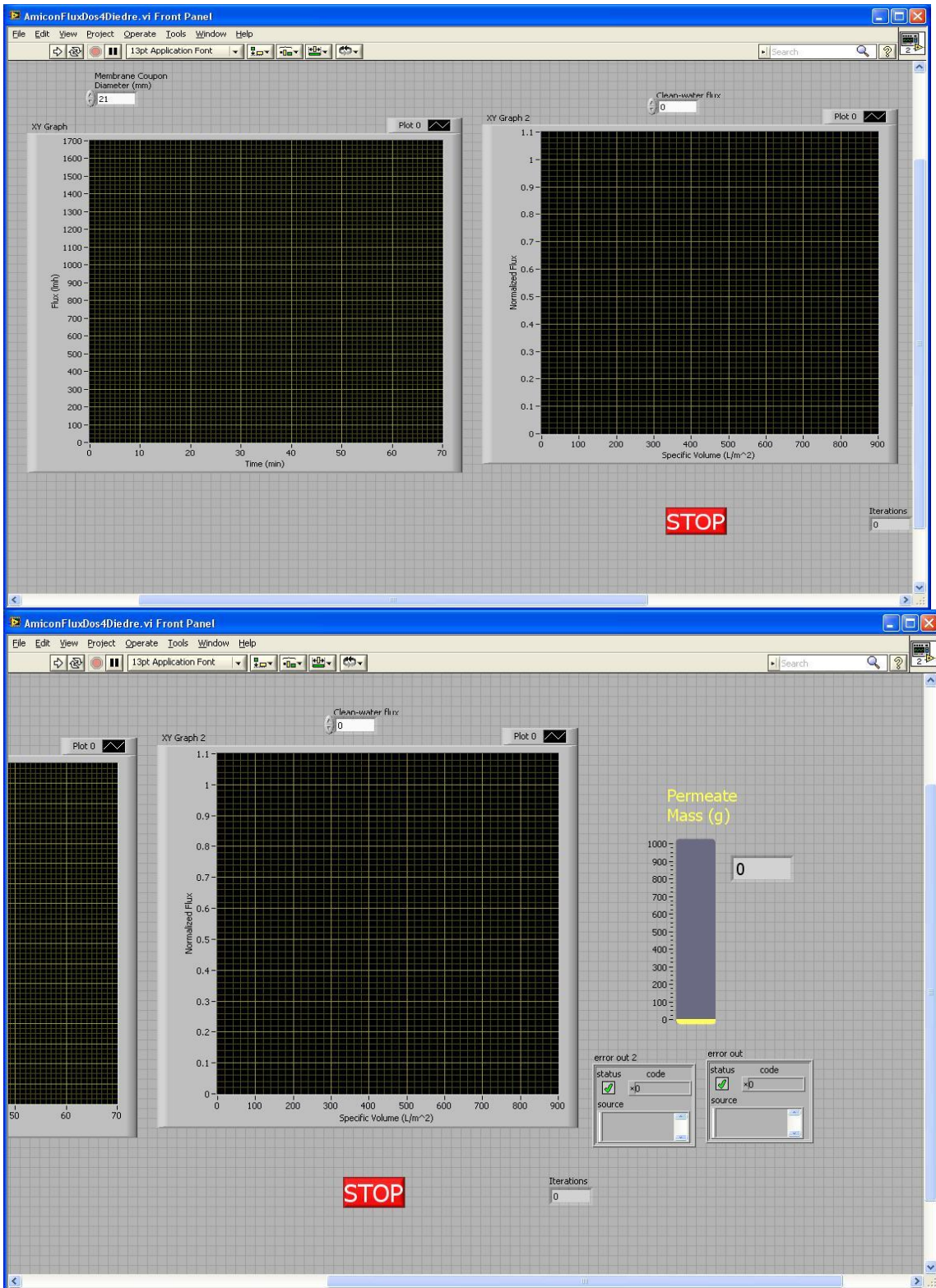


Figure A3 The Panel of Labview

APPENDIX E: The Correlation between Suwannee River NOM Concentration and TOC

As mentioned in Section 4.3.2, the powdered SRNOM was diluted with DDI to get a series of concentration: 0.5 mg/L, 1 mg/L, 3 mg/L, 4 mg/L, 5 mg/L, 10 mg/L, 15mg/L 20 mg/L. UV/Vis spectrophotometer was applied to get a calibration curve between adsorbance and concentration. The same set of samples were used in TOC analyzer to obtain the corresponding TOC value. The calibration curves and correlations were shown in Figure A4, Figure A5, and Figure A6. From Figure A4, when TOC is 4 mg/L, the NOM concentration is 10 mg/L.

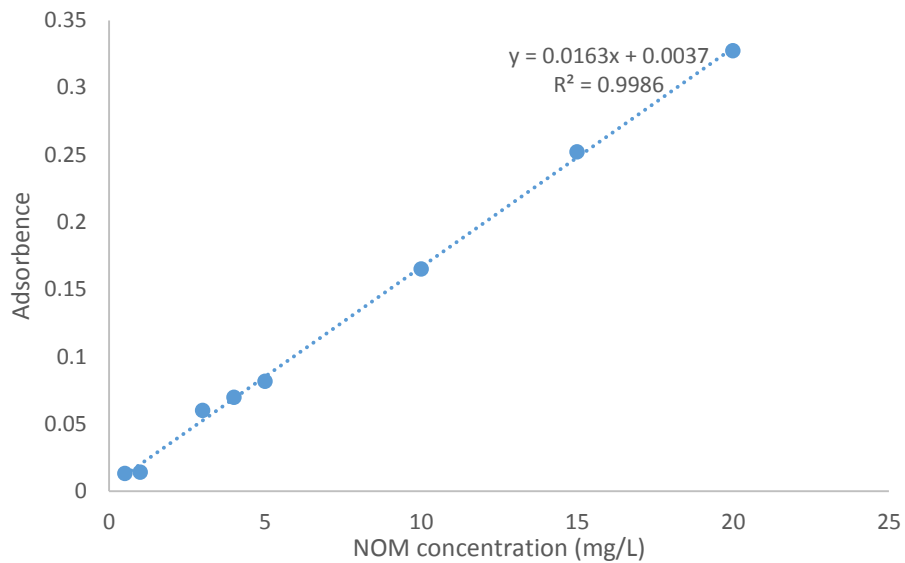


Figure A4 The calibration curve of SRNOM between concentration and Adsorbance

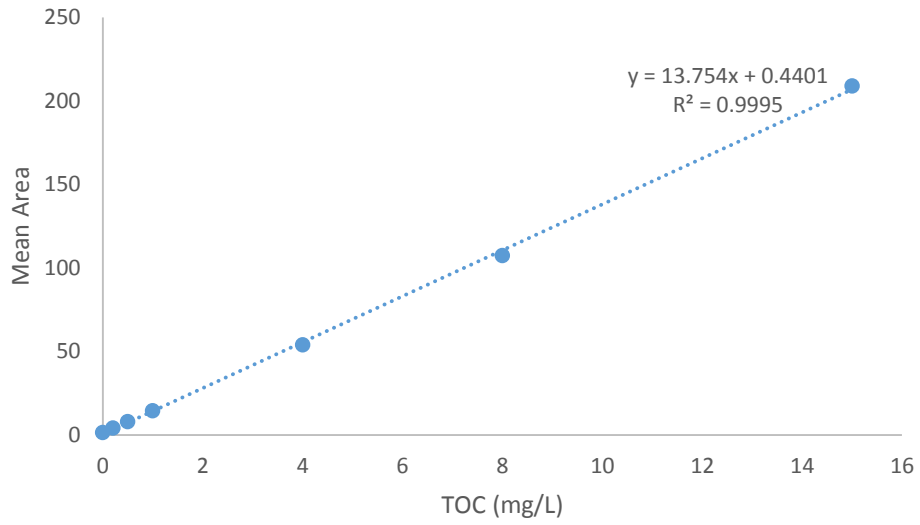


Figure A5 The calibration curve of TOC value

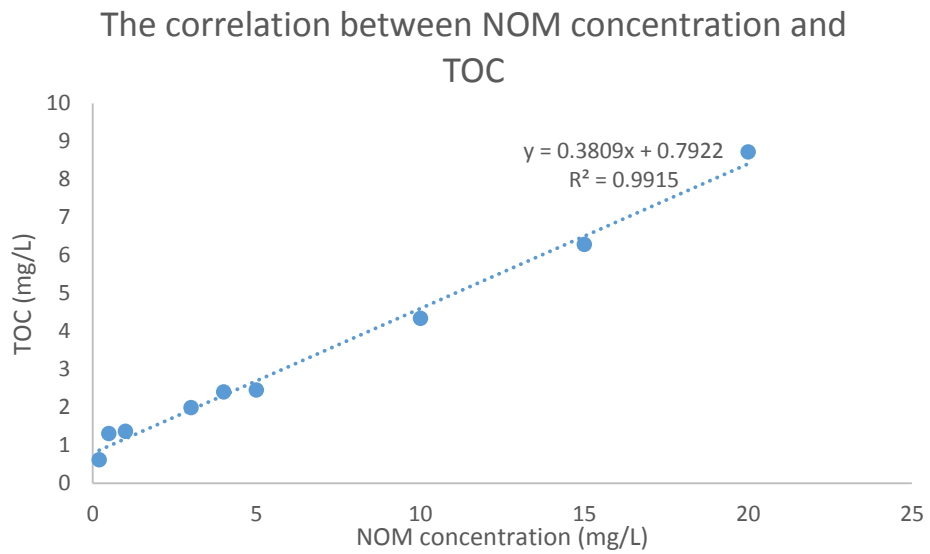


Figure A6 The correlation between NOM concentration and TOC

APPENDIX F: Preparation and Storage of Standard Solutions

Preparation of TOC Standard Solutions:

1. Accurately weigh 2.125g of reagent grade potassium hydrogen phthalate previously dried at 105-120°C for about 1 hour and cooled in a desiccator.
2. Transfer to 1L volumetric Flask and dissolve in DDI water (Glass Bottle).
3. Add DDI water to the 1L mark, and stir the solution.

The carbon Concentration of the solution corresponds to 1000mg C/L (1000mg C/L = 1000ppm C). This solution is retained as the standard stock solution.

4. The standard stock solution is diluted with DDI water to prepare standard solutions at the required concentrations.

Preparation of TN Standard Solutions:

1. Accurately weigh 7.219g of special reagent grade potassium nitrate dried for 3 hours at 105-110°C and cooled in a desiccator.
2. Transfer the weighed material to a 1 L volumetric flask (Plastic Bottle).
3. Add DDI water to the 1L mark.
4. Stir well to mix.
5. This solution corresponds to 1000mg N/L (=1000ppm N) and is referred to below as “TN Standard Solution”.
6. The standard stock solution is diluted with DDI water to prepare standard solutions at the required concentrations.

Storage of Standards:

- Standard solutions must be kept at 5°C for no more than a month.

DILUTION OF STOCK SOLUTIONS

Need:

- TOC and TN stock solutions (Placed in the fridge).
- Volumetric flasks (Plastic and Glass) (Box in the lab on shelves).
- One rubber nipple.
- Four glass pipets.

Calculations:

- All dilutions are done by mass.

$$X \text{ ml} \times (1000\text{mg/L}) = (100\text{mg/L}) \times (100\text{ml})$$

$$\text{Unknown Amount} \times \text{Stock Solution} = \text{Target Conc.} \times \text{Vol. of Glassware}$$

$$X = 10\text{ml}$$

- Since density of solution is approximately that of pure water.

$$10\text{ml} \times (1\text{g/ml}) = \underline{10\text{g}}$$

- So for all dilutions;

For TOC;

- Take 10g stock solution and then dilute by adding DDI water in a 100ml volumetric flask to obtain 100ppm solution.

Table A1 Preparation of TOC stock solution

Target Concentration (ppm)	Used Stock Solution (ppm)	Add stock solution depending on the volume of volumetric flask.			
		Volume of Volumetric Flask (ml)	Added Amount (g)	Volume of Volumetric Flask (ml)	Added Amount (g)
0.2	100	200	0.40	250	0.50
0.5	100	200	1.00	250	1.25
1	100	200	2.00	250	2.50
2	100	200	4.00	250	5.00
4	1000	200	0.80	250	1.00
8	1000	200	1.60	250	2.00
15	1000	200	3.00	250	3.75
25	1000	200	5.00	250	6.25

For TN;

- Take 10g stock solution and then dilute by adding DDI water in a 100ml volumetric flask to obtain 100ppm solution.

Table A2 Preparation of TN stock solution

Target Concentration (ppm)	Used Stock Solution (ppm)	Add stock solution depending on the volume of volumetric flask.			
		Volume of Volumetric Flask (ml)	Added Amount (g)	Volume of Volumetric Flask (ml)	Added Amount (g)
0.4	100	200	0.80	250	1.00
0.8	100	200	1.60	250	2.00
1.2	100	200	2.40	250	3.00
2.4	100	200	4.80	250	6.00
5	1000	200	1.00	250	1.25
10	1000	200	2.00	250	2.50
25	1000	200	5.00	250	6.25

Important notes:

- Make sure to shake out any liquid in containers prior to dilutions.
- Do NOT use containers for other purposes; Containers do not need to be washed, rinse them well with DDI water.

REFERENCES

1. Focazio, M.J.; Kolpin, D.W.; Barnes, K.K.; Furlong, E.T.; Meyer, M.T.; Zaugg, S.D.; Barber, L.B.; Thurman, M.E. A national reconnaissance for pharmaceuticals and other organic wastewater contaminants in the United States – II) Untreated drinking water sources. *Science of Total Environment*. 2008, 402, 201-216.
2. Sullivan, P.J.; Agardy, F.J.; Clark, J.J. *The Environmental Science of Drinking Water*; Elsevier: Burlington, MA, 2005.
3. O'Connor, J.T.; O'Connor, T.; Twait, R. *Water Treatment: Plant Performance Evaluations and Operations*; Wiley and Sons: Hoboken, NJ, 2009.
4. Lee, S.J.; Choo, K.H.; Lee, C.H. Conjunctive use of ultrafiltration with powered acitvated carbon adsorption for removal of synthetic and natural organic matter. *Journal of Industrial and Engineering Chemistry*. 2000, 6, 357-364.
5. Fitzer, E.; Köchling, K.H.; Boehm, H.P.; Marsh, H. Recommended terminology for the description of carbon as a solid. *Pure and Applied Chemistry*. 1995, 67, 473-508.
6. Muller, E.A.; Gubbins, K.E. Molecular simulation study of hydrophilic and hydrophobic behavior of activated carbon surfaces. *Carbon*. 1998, 36, 1433-1438.

7. Okada, K.; Yamamoto, N.; Kameshima, Y.; Yasumori, A. Porous properties of activated carbons from waste newspapers prepared by chemical and physical activation. *Journal of Colloid and Interface Science*. 2003, 262, 179-193.
8. Wu, F.C.; Tseng, R.L.; Juang, R.S. Adsorption of dyes and phenols from water on the activated carbons prepared from corncob wastes. *Environmental Technology*. 2001, 22, 205-213.
9. Marsh, H.; Rodríguez-Reinoso, F. *Activated Carbon*; Elsevier Ltd.: Oxford, UK, 2006.
10. Sontheimer, H.; Crittenden, J.C.; Summers, R.S. *Activated Carbon for Water Treatment*; American Water Works Association, 1988.
11. Karanfil, T.; Kilduff, J.E. Role of granular activated carbon surface chemistry on the adsorption of organic pollutants. 1. Priority pollutants. *Environmental Science and Technology*. 1999, 33, 3217-3224.
12. Müller, E.A.; Gubbins, K.E. Molecular simulation study of hydrophilic and hydrophobic behavior of activated carbon surfaces. *Carbon* 1998, 36, 1433-1438.
13. Julien, F.; Baudu, M.; Mazet, M. Relationship between chemical and physical surface properties of activated carbon. *Water Research*. 1998, 32, 3414-3424.
14. Semmens, M.J.; Norgaard, G.E.; Hohenstein, G.; Staples, A.B. Influence of pH on the removal of organics by granular activated carbon. *Journal- American Water Works Association*. 1986, 78, 89-93.

15. Knappe, D.R.U.; Matsui, Y.; Snoeyink, V.L.; Roche, P.; Prados, M.J.; Bourbigot, M.M. Predicting the capacity of powdered activated carbon for trace organic compounds in natural waters. *Environmental Science and Technology*. 1998, 32, 1694-1698.
16. Najm, I.N.; Snoeyink, V.L.; Richard, Y. Effect of initial concentration of a SOC in natural water on its adsorption by activated carbon. *Journal- American Water Works Association*. 1991, 83, 57-63.
17. Li, Q.; Snoeyink, V.L.; Marinas, B.J.; Campos, C. Elucidating competitive adsorption mechanisms of atrazine and NOM using model compounds. *Water Research*. 2003, 37, 773-784.
18. Newcombe, G.; Morrison, J.; Hepplewhite, C.; Knappe, D.R.U. Simultaneous adsorption of MIB and NOM onto activated carbon: II. Competitive effects. *Carbon*. 2002, 40, 2147-2156.
19. Hopman, R.; Siegers, W.G.; Kruithof, J. C. Organic micropollutant removal by activated carbon fiber filtration. *Water Supply*. 1995, 13 (3-4), 257-261.
20. Ding, L.; Snoeyink, V.L.; Mariñas, B.J.; Yue, Z.; Economy, J. Effects of powdered activated carbon pore size distribution on the competitive adsorption of aqueous atrazine and natural organic matter. *Environmental Science and Technology*. 2008, 42, 1227-1231.

21. Ando, N.; Matsui, Y.; Kurotobi, R.; Nakano Y.; Matsushita, T.; Ohno, K. Comparison of natural organic matter adsorption capacities of super-powdered activated carbon and powdered activated carbon, *Water Research*. 2010, 44, 4127–4136.
22. Matsui, Y.; Ando, N.; Sasaki, H.; Matsushita, T.; Ohno, K. Branched pore kinetic model analysis of geosmin adsorption on super-powdered activated carbon. *Water Research*. 2009, 43, 3095-3103.
23. Matsui, Y.; Nakao, S.; Yoshida, T.; Taniguchi, T.; Matsushita, T. Natural organic matter that penetrates or does not penetrate activated carbon and competes or does not compete with geosmin. *Separation and Purification Technology*. 2013, 113, 75-82.
24. Anonymous. *United States Federal Register*. 1998, 63(241), 69390-69476.
25. Zularisam, A.W.; Ismail, A.F.; Salim, R. Behaviours of natural organic matter in membrane filtration for surface water treatment – a review. *Desalination*. 2006, 194, 211-231.
26. Yuan, W.; Zydney, A.L. Humic acid fouling during microfiltration. *Journal of Membrane Science*. 1999, 157, 1-12.
27. Leenheer, J.A. Chemistry of dissolved organic matter in rivers, lakes and reservoirs. *Journal- American Chemical Society*. 1994, 237, 196-221.
28. Stevenson, F.J. *Humus Chemistry*. Wiley, New York, 1982.

29. Matilainen, A.; Vepsalainen, M.; Sillanpaa, M. Natural organic matter removal by coagulation during drinking water treatment: A review. *Advances in Colloid and Interface Science*. 2010, 159, 189-197.
30. Eikebrokk, B.; Vogt, R.D.; Liltved, H. NOM increase in Northern European source waters: discussion of possible causes and impacts on coagulation/contact filtration processes. *Water Science and Technology*. 2004, 4 (4).
31. Christensen, M., Ed. *Microfiltration and Ultrafiltration Membranes for Drinking Water – Manual of Water Supply Practices*. 1st Ed.; American Water Works Association: Denver, CO, 2005.
32. Williams, J.; Goel, R.; Flora, J.; Vidic, R. Investigating role of growing adsorbent bed in a dead-end PAC/UF process. *Journal of Environmental Engineering*. 2005, 131, 1583-1588.
33. Yiantios, S.; Karabelas, A. An experimental study of humic acid and powdered activated carbon deposition on UF membranes and their removal by backwashing. *Desalination*, 2001, 140, 195.
34. Campos, C.; Mariñas, B.J.; Snoeyink, V.L.; Baudin, I.; Láiné, J.M. PAC-membrane filtration process. I: Model development. *Journal of Environmental Engineering*. 2000, 126, 98-103.

35. Campos, C.; Mariñas, B.J.; Snoeyink, V.L.; Baudin, I.; Laine, J.M. Adsorption of trace organic compounds in CRISTAL® processes. *Desalination* 1998, 117, 265-271.
36. Oh, H.; Yu, M.; Takizawa, S.; Ohgaki, S. Evaluation of PAC behavior and fouling formation in an integrated PAC-UF membrane for surface water treatment. *Desalination* 2006, 192, 54-62.
37. Campinas, M.; Rosa, M.J. Assessing PAC contribution to the NOM fouling control in PAC/UF systems. *Water Research*. 2010, 44, 1636-1644.
38. Mozia, S.; Tomaszewcka, M.; Morawski, A. Studies on the effect of humic acids and phenol on adsorption-ultrafiltration process performance. *Water Research*. 2005, 39, 501-509.
39. Lin, C.F.; Huang, Y.J.; Hao, O.J. Ultrafiltration processes for removing humic substances: effect of molecular weight fractions and PAC treatment. *Water Research*. 1999, 22, 1252-1264.
40. Li, Q.; Snoeyink, V.L.; Mariñas, B.J.; Campos, C. Pore blockage effect of NOM on atrazine adsorption kinetics of PAC: the roles of PAC pore size distribution and NOM molecular weight. *Water Research*. 2003, 37, 4863-4872.
41. Thiruvengkatachari, R.; Shim, W.; Lee, J.; Aim, R.; Moon, H.; A novel method of powdered activated carbon (PAC) pre-coated microfiltration (MF) hollow fiber

- hybrid membrane for domestic wastewater treatment. *Colloids and Surfaces A*. 2006, 274, 24-33.
42. Heijman, S.G.J.; Hamad, J.Z., Kennedy, M.D.; Schippers, J.; Amy, G. Submicron powdered activated carbon used as a pre-coat in ceramic microfiltration. *Desalination and Water Treatment* 2009, 9, 86-91.
 43. Campos, C.; Baudin, I.; Lainle, J.M. Adsorption performance of powdered activated carbon ultrafiltration systems. *Proceedings of the Conference on Membranes in Drinking and Industrial Water Production*. 2000, 1, 189–195.
 44. Campos, C.; Marinas, B.J.; Snoeyink, V.L.; Baudin, I.; Lainle, J.M. Adsorption of trace organic compounds in CRISTAL® processes. *Desalination*. 1998, 117, 265–271.
 45. Lee, S.J.; Choo, K.H.; Lee, C.H. Conjunctive use of ultrafiltration with powdered activated carbon adsorption for removal of synthetic and natural organic matter. *Journal of Industrial and Engineering Chemistry*. 2000, 6, 357-364.
 46. Juang, R.S.; Lee, W.C.; Chen, C.L. Removal of sodium dodecyl benzene sulfonate and phenol from water by a combined PAC adsorption and cross-flow microfiltration process. *Journal of Chemical Technology and Biotechnology*. 2004,79, 240–246

47. Najm, I.N.; Snoeyink, V.L.; Suidan, M.T.; Lee, C.H.; Richard, Y. Effect of particle size and background natural organics on the adsorption efficiency of PAC. *Journal- American Water Works Association*. 1990, 82, 65-72.
48. Mozia, S.; Tomaszewska, M. Treatment of surface water using hybrid processes--adsorption on PAC and ultrafiltration. *Desalination*. 2004, 162, 23-31.
49. Hong, S.; Elimelech, M. Chemical and physical aspects of natural organic matter (NOM) fouling of nanofiltration membranes. *Journal of Membrane Science*. 1997, 132, 159.
50. Yuan, W.; Zydney, A.L. Effects of solution environment on humic acid fouling during microfiltration. *Desalination*. 1999, 122, 63.
51. Schafer, A.I.; Schwicker, U.; Fishcher, M.M.; Fane, A.G.; Waite, T.D. Microfiltration of colloids and natural organic matter. *Journal of Membrane Science*. 2000, 171, 151.
52. Amy, G.; Cho, J. Interactions between natural organic matter (NOM) and membranes: rejection and fouling. *Water Science and Technology*. 1999, 40, 131.
53. Braghetta, A.; DiGiano, F.A.; Ball, W.P. NOM accumulation at NF membrane surface: impact of chemistry and shear. *Journal of Environmental Engineering-ASCE*. 1998, 1087.

54. Jucker, C.; Clark, M.M. Adsorption of aquatic humic substances on hydrophobic ultrafiltration membranes. *Journal of Membrane Science*. 1994, 97,37.
55. Jones, K.L.; O'Melia, C.R. Protein and humic acid adsorption onto hydrophilic membrane surfaces: effects of pH and ionic strength. *Journal of Membrane Science*. 2000, 165, 31.
56. Lin, C.F.; Huang, Y. J.; Hao, O.J. Ultrafiltration processes for removing humic substances: effect of molecular weight fractions and PAC treatment. *Water Research*. 1999, 33, 1252-1264.
57. Li, Q.; Elimelech, M. Natural organic matter fouling and chemical cleaning of nanofiltration membranes. *Water Science and Technology*. 2004, 4, 245-251.
58. Costa, A.R.; Pinho, M.N.; Elimelech, M. Mechanisms of colloidal natural organic matter fouling in ultrafiltration. *Journal of Membrane Science*. 2006, 281, 716-725.
59. Pelekani, C.; Snoeyink, V. L., Competitive adsorption between atrazine and methylene blue on activated carbon: the importance of pore size distribution, *Carbon* 2000, 38, 1423-1436.
60. Cho. J.; Amy, G.; Pellegrino, J. Membrane filtration of natural organic matter: initial comparison of rejection and flux decline characteristics with ultrafiltration and nanofiltration membranes. *Water Research*. 1999, 33, 2517-2526.

61. Fan, L.H.; Harris, J.L.; Roddick, A.F.; Booker, N.A. Influence of the characteristics of natural organic matter on the fouling of microfiltration membranes. *Water Research*. 2001, 35, 4455-4463.
62. Lee, N.; Amy, G.; Croue, J.P.; Buisson, H. Identification and understanding of fouling in low-pressure membrane (MF/UF) filtration by natural organic matter (NOM). *Water Research*. 2004, 38, 4511-4523.
63. Seidel, A.; Elimelech, M. Coupling between chemical and physical interactions in natural organic matter (NOM) fouling of nanofiltration membranes: implications for fouling control. *Journal of Membrane Science*. 2002, 203, 245-255.
64. Ellerie, J.R., Carbonaceous adsorbents as coatings for ultrafiltration membranes., in *Environmental Engineering and Science*. 2012, Clemson University. p. 35.
65. Colombini, M.P.; Fuoco, R.; Giannarelli, S.; Pospisil, L.; Trskova, R. Protonation and degradation reactions of s-triazine herbicides. *Microchemical Journal*. 1998, 59, 239-245.
66. Technical Factsheet on: Atrazine.

<http://water.epa.gov/drink/contaminants/basicinformation/atrazine.cfm>
67. Ellerie, J.R.; Apul, O.G.; Karanfil, T.; Ladner, D.A. Comparing graphene, carbon nanotubes, and superfine powdered activated carbon as adsorptive coating

materials for microfiltration membranes. *Journal of Hazardous Materials*, 2013. 261(0): p. 91-98.

68. Drinking Water Treatability Database.

<http://iaspub.epa.gov/tdb/pages/treatment/treatmentOverview.do?treatmentProcessId=2074826383>

69. Adam, L.; Grzesiak; Meidong, L.; Kibum, K.; Adam, J. Comparison of the for anhydrous polymorphs of carbamazepine and the crystal structure of form I, *Journal of Pharmaceutical Sciences*. 2003, 92,11.
70. Sontheimer, H.; Crittenden, J.C.; Summers, R.S. *Activated Carbon for Water Treatment*, second ed. DVGW-Forschungsstelle, Karlsruhe, Germany, 1988.
71. Matsushita, T.; Suzuki, H.; Shirasaki, N.; Matsui, Y.; Ohno, K. Adsorption virus removal with super-powdered activated carbon. *Separation and Purification Technology*. 2013, 107, 79-84.
72. Wu, H.W.; Xie, Y.F. Effects of EBCT and water temperature on HAA removal using BAC. *Journal - American Water Works Association*. 2014, 97, 94-101.
73. Knappe, D.R.U.; Snoeyink, V.L.; Roche, P.; Prados, M.J.; Bourbigot, M.M. The effect of preloading on rapid small-scale column test predictions of atrazine removal by GAC adsorbers. *Water Research*. 1997, 31 (11), 2899-2909.

74. Matsui, Y.; Hasegawa, H.; Ohno, K.; Matsushita, T.; Mima, S.; Kawase, Y.; Aizawa, T. Effects of super-powdered activated carbon pretreatment on coagulation and trans-membrane pressure buildup during microfiltration. *Water Research*. 2009, 43, 5160-5170.
75. Ando, N.; Matsui, Y.; Kurotobi, R.; Nakano, Y.; Matsushita, T.; Ohno, K.; Ohno, K. Comparison of natural organic matter adsorption capacities of super-powdered activated carbon and powdered activated carbon. *Water Research*. 2010, 44, 4127-4136.
76. Matsui, Y.; Yoshida, T.; Nakao, S.; Knappe, D.; Matsushita, T. Characteristics of competitive adsorption between 2-methylisoborneol and natural organic matter on superfine and conventionally sized powdered activated carbons. *Water Research*. 2012, 46, 4741 -4749.
77. Bjelopavlic, M.; Newcombe, G.; Hayes, R. Adsorption of NOM onto activated carbon: effect of surface charge, ionic strength, and pore volume distribution. *Journal of Colloid and Interface Science*. 1999, 210, 271-280.
78. Bakkaloglu, S. Superfine powdered activated carbon adsorption on synthetic organic chemicals compared to powdered activated carbon, in *Environmental Engineering and Science*. 2014, Clemson University.